ALMA MATER STUDIORUM - UNIVERSITÀ DI BOLOGNA

FACOLTA' DI INGEGNERIA

Corso di Laurea in Ingegneria Civile

Dipartimento: D.I.S.T.A.R.T. Indirizzo: Strutture

TESI DI LAUREA

in
Progetti di strutture

SYSTEM IDENTIFICATION OF A FOOTBRIDGE IN IMOLA

Tesi di laurea di:

MADDALENA DALL'AGATA

Relatore:

Ill.mo Prof. MARCO SAVOIA

Correlatori:

Ill.mo Prof. RAIMONDO BETTI
Ing. LORIS VINCENZI

Sessione I

Anno Accademico 2008-2009

Quello che noi facciamo è
solo una goccia nell'oceano,
ma se non lo facessimo
l'oceano avrebbe una goccia
in meno.

S.T.di Calcutta

Introduction

This work is aimed at the system identification of a footbridge in Imola. The system identification essentially consists of study of the dynamic properties and of the creation and the calibration of a mechanical model basing on dynamic tests in field. The diffusion of this method was really important in the last years because it gives the possibility to obtain the dynamical characterization of structures using non-destructive methods. Thinking about the deteriorating of brick wall or cables in bridge it is clear why it is do important to know the actual proprieties and behaviour of structure. In order to get these information, dynamic forces are applied to the structure (vibration generator consisting of closed-loop electro-mechanic actuator, traffic, wind, etc…), and the measured data are analyzed by identification techniques in the time and in the frequency domain, at this point the output signals obtained are compared with the model that has to be calibrated.

The first aim of this work therefore is to analyze the outputs measured by the accelerometers with the EFDD (Enhance Frequency Domain Decomposition) and to derivate an accurate mechanical model of the footbridge under examination comparing it with the results derived from the analysis.

The mechanical model of a bridge, a finite element (FE) model in the case majority, is usually defined on the basis of highly idealized engineering designs that may or may not truly represent the actual behaviour of the structure under study. In fact, when static or dynamic tests are performed to validate the analytical model of a bridge, inevitably some discrepancies arise between the experimental results, typically expressed in terms of static deflections or natural frequencies and mode shapes, and their analytical counterparts. Large deviations between the experimental and analytical values could be responsible for significant differences between the actual and calculated capacities of a bridge. Moreover, an inaccurate mathematical model of a bridge cannot be reliably used as a baseline for future damage assessment applications. The experimental techniques are nowadays developed to a high degree of sophistication, but the interpretation of measurements often presents intrinsic difficulties. In fact, in recent years, there has been an increasing interest in the civil

and mechanical engineering community in methodologies that are capable of getting dynamic properties.

Modal parameter identification is one of the most common procedures to identify dynamic properties of a vibrating structure starting from modal tests. Modal parameters can be estimate from a variety of different measurements in different data domains (time and/or frequency domain). These measurements can include free-decays, forced responses, frequencies response functions or impulse response functions. In fact Acceleration records at different frequencies are used to calculate the corresponding FRFs. From these, frequencies domain methods can be used to identify frequencies, deformations and damping ratios of various modes. The forces exciting the structures can be divided in two principal categories: the ambient and the artificial forces. The second have the advantage that , especially for mechanical system, it is possible to regulate, impose, measure and check the motion of the structure, but the disadvantage to need the interruption of the exercise in order to do the tests The ambient excitation in the contrary takes the advantage not to interrupt the common use of the structure.T he measurements can be generated with no measured inputs, single measured input or multiple measured inputs.

Most current modal parameter estimation techniques are based on the frequency response function (FRF) or, equivalently, impulse response function (IRF) obtained from the measured data. FRFs are typically found by Fast Fourier Transform.

The simplest approach to estimate the modal parameters of a structure is the so-called *Peak-Picking* (*PP*) method. The method's name refers to the fact that the identification of the Eigen frequencies is found picking peaks from a spectrum plot. Probably due to its simplicity, it is one of the most widely used methods in civil engineering. Method details are, for instance, discussed in [Bendat & Piersol, 1993]. It assumes that the damping is low and that the modes are well-separated. A violation of these assumptions leads to erroneous results. In fact, the method identifies the *operational deflection shapes* instead of mode shapes and for closely-spaced modes such an operational deflection shape will be the superposition of multiple modes. Other disadvantages are that the selection of the Eigen frequencies can become a subjective task if the spectrum peaks are not very clear or if the frequency resolution is not fine

enough. Methods that elude these problems are the FDD and EFDD. They use the Singular Value Decomposition method diagonalizing the spectral matrix and decomposing it into a set of auto spectral density functions, each corresponding to a Single Degree of Freedom (SDOF) system. The Enhanced Frequency Domain Decomposition (EFDD) is basically an extension of the FDD technique capable of providing damping information. In EFDD, the identified frequency function around each resonant peak is transferred back to the time domain using Inverse Discrete Fourier and damping can be obtained by the logarithmic decrement of the correspond SDOF normalized autocorrelation function. This is the approach we used for our case of study. The results are right if the structure has a low damping, the load is really a white noise and the mode shapes of the matched modes are orthogonal. Otherwise they are approximated but good anyway. To have more information about identification techniques both in the time and in the frequency domain we remand to the third chapter. The estimation of the modal parameters starting from output measurements only (e.g. accelerations) is known as *stochastic system identification,* where the structure is excited by an un-measurable input force. In these methods, deterministic knowledge of inputs is replaced by the assumption that the input is a realization of a stochastic process (white noise).

In the following chapters they are presented the results of an application of structural identification based on dynamic data for a one span footbridge, with a slab-on-beams deck, stayed-cable type, recently built in the new road axis in Pedagna, Imola. In this work it is used, as we said, an identification technique and it is create an almost accurate model representing the real behaviour and improving the fitting between the prediction of a FE model and the real structural behaviour.

In the first chapter the main characteristics of the cable-stayed bridges and some bibliography about the FE model are reported. Moreover also a detailed description of the real and of the FE model footbridge are reported.

In the second chapter the dynamic theory of a single degree and a multi degree of freedom systems are recalled. Also the signals analysis and the tread of the signals, such as filtering, windowing, overlapping techniques are explained.

In the third chapter there is a wide explanation of the EFDD method used to analyse the measured data showing by steps how the method works.

In the fourth chapter the process of static tests are reported and it focuses on the validation of the FE model comparing and calibrating it with output from the tests. The instruments of measure used to get the data are also shown.

The fifth chapter is the most important and all the dynamic results are contained in it. Forced-vibration tests were conducted to extract the dynamic parameters of the first modes of vibration. The identification procedure based on modal analysis and FE modelling is presented for the characterization of the footbridge. Also the theory of the cable is reported.

The resulting calibrated model will be of valuable importance for new structural identifications in the same bridge giving the possibility to identify and localize eventually future damages in the footbridge.

Introduzione

Questo lavoro tratta l'identificazione strutturale di una passerella pedonale costruita in Imola. L'identificazione strutturale consiste nel ricavare le caratteristiche dinamiche della struttura e nel creare un modello meccanico e calibrarlo con i dati sperimentali analizzati provenienti da prove dinamiche realizzate in sito. Questa tecnica si è diffusa ampiamente negli ultimi anni proprio perché dà la possibilità di ricavare le caratteristiche dinamiche e quindi di conoscere il comportamento della struttura caso di studio usando prove non distruttive. Se si pensa al degrado delle strutture in muratura o dei cavi in acciaio nei ponti sospesi o strallati si intuisce l'importanza di conoscere l'attuale stato di tali strutture in modo anche da poterlo monitorare. Per poter ricavare le caratteristiche dinamiche delle strutture occorre applicare carichi dinamici (vibrodina, traffico, rilascio di blocchi di cemento, carichi impulsivi, corse, etc…) e i dati registrati (abbassamenti, accelerazioni…) vengono analizzati tramite un algoritmo d'identificazione ed infine le caratteristiche dinamiche ottenute vengono comparate con quelle risultanti dal modello.
L'obbiettivo primario di questo lavoro è quello di analizzare i dati registrati dagli accelerometri tramite la tecnica d'identificazione chiamata EFDD (Enhance Frequency Domain Decomposition) e di derivare un modello rispettoso della situazione reale.
Per questo è stato creato un modello agli elementi finiti tramite il programma di calcolo Straus7.

Il modello meccanico, spesso un modello agli elementi finiti è di solito definito sulla base di una idealizzazione del progetto ingegneristico che può o meno essere rappresentativo dell'attuale stato della struttura in esame. Infatti, quando tests statici o dinamici sono effettuati, inevitabilmente si rivela una certa discrepanza tra i dati sperimentali espressi in termini di abbassamenti o frequenze naturali e quelli analitici. Grandi deviazioni tra i dati sperimentali e analitici, possono essere responsabili di discrepanze significative tra i valori di capacità della struttura reali e quelli aspettati. Inoltre, un modello matematico inaccurato del ponte non può essere usato come linea guida nello studio di futuri danneggiamenti. Le tecniche sperimentali sono oggi

migliorate e hanno raggiunto un livello molto alto di sofisticazione, ma l'interpretazione dei dati raccolti presenta spesso intrinseche difficoltà. Infatti, negli ultimi anni, c'è stato un incremento d'interesse nelle comunità civili e meccaniche riguardo a metodologie capaci di ricavare le proprietà dinamiche delle strutture.

L'identificazione dei parametri modali è una delle più comuni procedure per identificare le proprietà dinamiche di una struttura in vibrazione partendo da prove modali. I parametri modali possono essere stimati da una vasta varietà di misure in differenti domini (dominio del tempo e/o delle frequenze). I dati possono includere vibrazioni libere, risposte di sistemi sforzati, risposte di funzioni in frequenza o funzioni di risposta impulsive. Le forze caratterizzanti eccitanti la struttura si dividono in due principali categorie: ambientali e forzate. I sistemi di eccitazione artificiale, in particolare i sistemi di tipo meccanico (es. vibrodina), hanno il vantaggio di poter imporre, misurare e controllare il moto della struttura, ma anche il grande svantaggio di richiedere l'interruzione dell'esercizio dell'opera per poter effettuare la prova.
L'utilizzo dell'eccitazione di tipo ambientale permette invece di eseguire le prove sulla struttura senza la necessità di interrompere il normale esercizio dell'opera durante le prove sperimentali. I dati misurati possono essere generati da input sconosciuto a singolo ingresso o ingresso multiplo.

La più comune tecnica di identificazione dei parametric modali è basata sulla risposta in frequanza (FRF) o, equivalentemente funzione di risposta impulsive (IRF) ottenuta dai dati sperimentali. Le FRFs sono tipicamente ottenute tramite trasformazione di Fourier.

Il metodo più semplice per la determinazione delle caratteristiche modali delle strutture nel dominio delle frequenze è il metodo *Peak-Picking* (*PP*). Il metodo prende nome dal fatto che la determinazione delle frequenze proprie è ottenuta dalla frequenza corrispondente ai picchi del modulo della *FRF*. Data la sua semplicità, nel passato questo metodo è stato il più diffuso per la determinazione delle caratteristiche modali di strutture civili [Bendat & Piersol, 1993]. Il metodo assume che lo smorzamento sia modesto e che i modi siano ben distinti tra loro. Nel caso in cui questo non accada, l'applicazione del metodo porta a commettere errori significativi. Infatti, il metodo identifica gli *operating deflection shape* invece dei modi propri,

ottenuti per somma di contributi di diversi modi propri. Un altro svantaggio di tale metodologia è dovuto alla necessità da parte dell'operatore di selezionare le frequenze proprie quando la FRF è definita con scarsa risoluzione o quando è presente un elevato livello di rumore nelle misure [Ewins, 2000].

I metodi FDD e EFDD eludono questo problema . Essi usano la decomposizione ai valori singolari diagonalizzando la matrice spettrale e decomponendola in una serie di funzioni di densità spettrale, ognuna corrispondente ad un sistema ad un singolo grado di libertà. L'EFDD è praticamente un'estensione della tecnica FFD ed è capace di ottenere frequenze proprie e rapporti di smorzamento. Nell'EFDD la funzione in frequenza identificata attorno al picco è trasferita di nuovo nel dominio del tempo usando la trasformata inversa di Fourier e il rapporto di smorzamento può essere ottenuto dal decremento logaritmico della corrispondente alla funzione normalizzata di autocorrelazione del sistema SDOF. Questa è la tecnica che viene usata nel presente lavoro ed in particolare ci si riferisce al caso di output only identification, dove l'input è assunto essere un processo stocastico (white noise). I risultati ottenuti dal metodo sono giusti se la struttura ha valori di smorzamento bassi, the i carichi sono veramente dei processi stocastici e se le forme modali sono ben separate e ortogonali. Altrimenti i risultati non saranno perfetti, ma comunque buoni. Per avere maggiori informazioni sulle diverse tecniche di identificazione nel dominio del tempo e delle frequenze ci si riferisca al capitolo terzo.

Nei paragrafi seguente sono presentati i risultati di una identificazione strutturale basata su prove dinamiche svolte su di una passerella pedonale strallata, con una luce principale, un pilone inclinato in cemento armato con camicia metallica collaborante, con impalcato formato da tubi in acciaio sostenenti una soletta di calcestruzzo e situata a Imola nel quartiere Pedagna. La tecnica di identificazione EFFD è stata usata e si è ottenuto un modello agli elementi finiti abbastanza accurato e in grado di riprodurre lo stato della passerella al momento delle prove.

Nel primo capitolo sono descritte le principali caratteristiche dei ponti strallati ed è introdotto il metodo agli elementi finiti. Inoltre sono riportate anche una descrizione dettagliata del caso in esame e del modello FE iniziale.

Nel secondo capitolo è introdotta l'analisi dinamica di sistemi ad un grado e a più gradi di libertà. Si spiega anche l'analisi e il trattamento del segnale, come il filtraggio, il finestra meno e la tecnica di sovrapposizione dei dati.

Nel terzo capitolo c'è un'ampia spiegazione della tecnica EFDD usata per analizzare i dati misurati e vengono mostrati i vari passaggi sequenziali del metodo.

Nel quarto capitolo sono riportate le prove dinamiche e i risultati ottenuti sono comparati con quelli del modello. Sono anche brevemente descritti gli strumenti utilizzati nelle prove.

Il quinto capitolo è il più importante, sono descritte le prove dinamiche, sono riportati i risultati derivanti dalla tecnica d'identificazione e i risultati sono comparati con quelli del modello. Esso è stato quindi calibrato. In questo capitolo viene riportata anche una breve introduzione alla non linearità dei cavi.

Chapter 1

2.1 Introduction

This study focuses on the System Identification of a footbridge in Imola (Italia). This footbridge is a cable stayed bridge, supported by three cables each part of the deck.

Typically a **cable-stayed bridge** is a bridge that consists of one or more columns (normally referred to as towers or pylons), in which cables that support the bridge deck are anchored. It is similar to a suspension bridge since both type of bridges have towers, cables and a suspended deck structure, but they differ for the way forces are transmitted from the deck to the towers(e.g. the disposition of the cables and the supports).

The deck of a suspension bridge merely hangs from the suspender, and has only to resist bending and torsion caused by live loads and aerodynamic forces. Contrarily, the deck in a cable-stayed bridge is in compression, pushed against the towers, and has to be stiff at all stages of construction and use. A great advantage is that cable stayed bridges are essentially made of cantilevers, and can be constructed by building out from the towers.

The suspension bridge has main cables suspended between towers, plus vertical suspender cables that carry the weight of the deck below, upon which traffic crosses. Cable-stayed bridges are divided in two classes depending on the disposition of the cables. In a **harp** configuration, the cables are made nearly parallel by attaching the cables at various points on the tower(s) so that the height of attachment of each cable on the tower is similar to the distance from the tower along the roadway to its lower attachment. In a **fan** design, the cables all connect to or pass over the top of the tower(s).

As a consequence of the cable geometry, suspension bridges need four anchorages to withstand the tension of the four cable-ends, while cable stayed bridges are self-anchored.

The cable-stay design is the optimum bridge for a span length between that of cantilever bridges and suspension bridges (between 500 and 2500 feet). Within this

range of span lengths a suspension bridge would require a great deal more cable, while a full cantilever bridge would require considerably more material and be substantially heavier. On the other hand, for very long spans (2500-7000 feet) a suspension bridge is more efficient. At some point, the towers for a cable-stayed bridge become too tall and have to carry to much weight.

2.2 Historical dissertation about the cable-stayed bridges

In the following section we are going to introduce a brief history of cable-stayed bridges.

The theoretical studies for the concept of a cable-stayed bridge have started in 1823 with Navier who visited the UK and studied the bridges being built there. There, combinations of suspended and cable-stayed bridges were built. In the following figure (1.1), it is shown in a very simply way how a cable-stayed bridge in the fan type of cables configuration works.

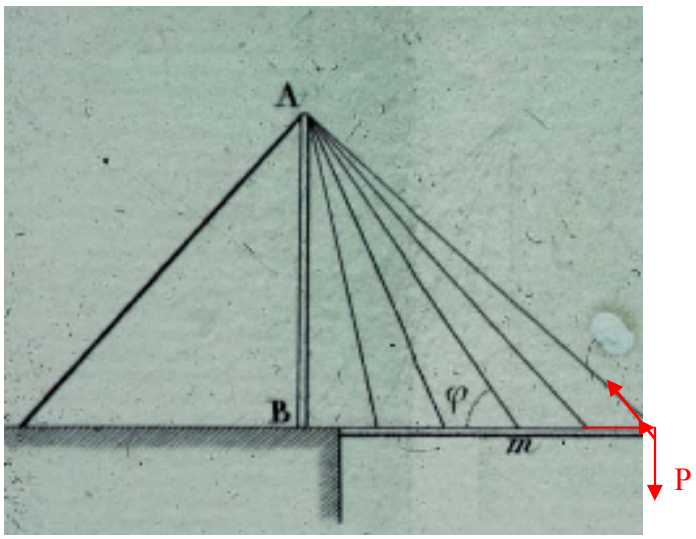

Figure1.1. Equilibrium in cable-stayed bridge

At equilibrium, the dead+live load P of the deck is taken by a tensile axial force in the cable stay and a compressive force in the deck.

Unfortunately a bridge built as a combination between the suspension and the cable stayed bridge collapsed a year after its public opening. This fact induced Navier to promote suspension bridges instead of cable-stayed bridges. Navier's studies were

very influential and this was one of the reasons that cable-stayed bridges did not materialize until 1955.

An other important engineer whose name is linked to cable-stayed bridges is Dischinger. He took part at a design competition where he proposed to design a cable stayed bridge, but lost. In any case, this was important because it brought back the idea of cable stays. Finally in a design competition in Sweden in 1955 for the Stromsund Bridge, Dischinger proposed a similar idea and won. The bridge is 332 m long, with a 182 m long span. It was opened in 1956, and it was the first large cable-stayed bridge in the world, constructed by Franz Dischinger, a pioneer in construction of cable-stayed bridges. The following picture (1.2) shows as the bridge looks today.

Figure1.2. A view of Stromsund Bridge in Sweden

The second step in the diffusion of this new typology of bridge construction came in 1958 in Dusseldorf, with the the design of bridges over the Rhine River. During WWII, all the bridges over the Rhine were destroyed except one and they had to be rebuilt. German designers adopted the cable-stayed form in some of the bridges.

Let us introduce now the first one built in the US: the Pasco-Kennewick Bridge over the Columbia River in Washington State. It is a fan-type form with all the cables emanating from essentially the same point. There was however a complication with construction since the point where all these cables emanate is difficult to build.

Figure1.3. A view of the Pasco-Kennewick Bridge

This type of bridge has a visual problem because the cables are not parallel and they do not create a harmonic look of the bridge. Such a look is, instead, apparent in the harp configuration, like the Second Strelasund Crossing in Germany.

Figure1.4. The Brotonne bridge by Jean Muller

The Brotonne bridge shown in figure 1.4, introduced some important innovations:

- ✓ The line of cables is in the middle of the roadway. Until now there were always two lines of cables, one on each side of the roadway.

- ✓ The deck is now cantilevered out of the middle line, in contrast in previous bridges it was simply supported.
- ✓ Because of the single line of cables, cluttering is avoided from any angle

Actually this is a hybrid cable configuration: between a fan and a harp.

There were a lot of other innovations and updating in cable stayed bridge, as they were increasing in number worldwide. These bridges are now built in more unusual styles for structural and aesthetic reasons (Rito 1996 and Menn 1996). Examples include the Lerez Bridge (Troyano et al. 1998) - a single inclined tower bridge; the Katsushika Harp Bridge (Takenouchi 1998) - having a single pylon and S shaped deck; the Marian Bridge (Kominek 1998) - having a single L shaped pylon; the Alamillo Bridge Casa 1995), with a single inclined pylon and the Safti Link Bridge (Tan 1996) – which has a curved deck and single offset pylon. The unique structural styles of these bridges beautify the environment but also add to the difficulties in accurate structural analysis.

2.3 Model Base Simulation

In order to study the footbridge a FEM model was created using a programming software called STRAU7. Such a model has been first developed using the design blueprints and then has been validated by comparing its dynamic characteristics with those extracted by experimental data.

In the following picture (1.5) is reported the steps of the Model Based Simulation.

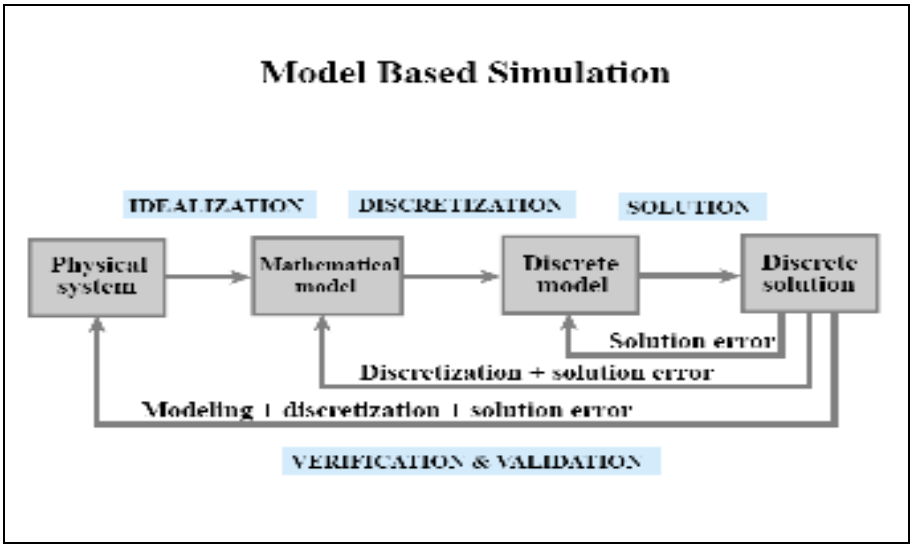

Figure1.5. Diagram of modelling steps

2.3.1 Idealization and Models

Idealization is a comprehensive term to indicate all the tools that an engineer uses to pass from the physical system to a mathematical model that conserves the main features of the real one. This is the most important step in engineering practice, because it cannot be "canned." It must be done by an engineer.

The word "model" has the traditional meaning of a scaled copy or representation of an object. And that is precisely how most dictionaries define it. We use here the term in a more modern sense, which has become increasingly common since the advent of computers:

A model is a symbolic device built to simulate and predict aspects of behaviour of a system.

Note the distinction made between *behaviour* and *aspects of behaviour*. To predict everything, in all physical scales, you must deal with the actual system. A model *abstracts* aspects of interest to the modeller.

The process is called *idealization* because the mathematical model is necessarily an abstraction of the physical reality and maintains just a number of the all aspects. The analytical or numerical results produced by the mathematical model are physically re-interpreted only for those aspects. To give an example of the choices that an engineer may face, suppose that the structure is a flat plate structure subjected to transverse loading. Here is a non-exhaustive list of four possible mathematical models:

1. A *very thin* plate model based on Von Karman's coupled membrane-bending theory;
2. A *thin* plate model which can be analysed using the classical approach of Kirchhoff's theory;
3. A *moderately thick* plate model which can be analysed by Mindlin-Reissner plate theory.
4. A *very thick* plate model which requires the three-dimensional elasticity.

The person responsible for this kind of decision is supposed to be familiar with the advantages, disadvantages, and range of applicability of each model. Furthermore the decision may be different in static analysis than in dynamics.

Engineering systems tend to be highly complex. For simulations it is necessary to reduce the complexity to manageable proportions. Mathematical modelling is an abstraction tool by which complexity can be controlled. This is achieved by "filtering out" physical details that are not relevant to the analysis process. Consequently, picking a mathematical model is equivalent to choosing an information filter.

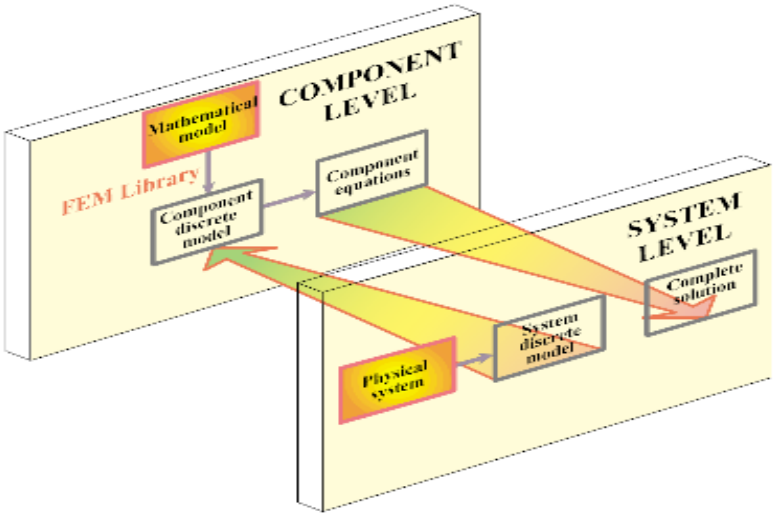

Figure1.6. The diagram is a simplification of engineering practice.

2.3.2 Discretization

Mathematical modelling is a simplifying step. Models of physical systems are not necessarily simple to solve. They often involve coupled partial differential equations in space and time subject to boundary and initial conditions. Such models might have an *infinite* number of degrees of freedom. Considering continuum mechanics problem degrees of freedom (DOFs) are the set of independent displacements and\or rotations that specify completely the displaced or deformed position and rotation of the system.

To solve the problem using a model there are two different types of procedures:

1. Using analytical solutions, also called "closed form solutions". They are useful particularly if they apply to a wide class of problems. Unfortunately they tend to be restricted to regular geometries and simple boundary conditions. Moreover some closed-form solutions, expressed for example as inverse of integral transforms, may have to be anyway numerically evaluated to be applied to a specific problem;

2. Using a numerical simulation. To make numerical simulations practical, it is necessary to reduce the number of degrees of freedom to a *finite* number. The reduction is called *discretization*. The product of the discretization process is the *discrete model*. For complex engineering systems this model is the product of a multilevel decomposition.

2.4 The Finite Element Method

The finite element method (FEM) is the more common discretization technique in structural mechanics. The FEM can be interpreted from either a physical or mathematical standpoint. The basic concept in the physical interpretation of FEM is the subdivision of the mathematical model into disjoint (non-overlapping) components of simple geometry called *finite elements* or *elements* for short. The response of each element is expressed in terms of a finite number of degrees of freedom characterized as the value of an unknown function, or functions, at a set of nodal points. The response of the mathematical model is then considered to be approximated by that of the discrete model obtained by connecting or assembling the collection of all elements. The paths of this Method consist of the following steps:

1. discretization: decomposition of the continue structure into piecewise elements;
2. definition of the unknown variables (e.g. displacements) at a finite number of points (nodes);
3. interpolation of the nodal values for each elements (approximation obtained by the shape function);
4. elements assemblage of the whole structure;
5. solution of the system obtaining the unknown variables(that consists of algebraic equations);
6. calculus of the secondary variables for each element (stress, strain,…).

2.5 STRAUS 7 (features of the program)

Straus7 is a general-purpose finite element analysis system consisting of pre-processor, solvers and post-processor.

The graphical environment in Straus7 includes advanced tools for the creation of finite element models, the application of loading and boundary conditions, direct interfaces to popular CAD and Solid Modelling systems, and automatic mesh generators. Post processing tools for the investigation of results include deformed displays, contour plots, point-and-click data inspection (peeking) and animation. The built-in report generator simplifies the task of compiling, printing and documenting results.

The solver includes basic Linear Static and Linear Buckling Analysis, a range of Dynamic Analysis solvers including direct and mode superposition solvers, advanced Nonlinear Static and Dynamic solvers and both Steady State and Transient Heat solvers.

2.5.1 Types of elements

In the following section the more important elements contained in the software and that we used to build the FEM model will be introduced.

- ✓ ***Beam*** is a generic name for a group of one-dimensional or line elements. These elements are all connected between two nodes at their ends and the single dimension is length.

In its most general form the beam element can carry axial force, shear force, bending moment and torque. In addition to the conventional beam element, there are a number of other special formulations of the beam element. (e.g. Spring / Damper, Cable, Truss, Cut-off bar, Point contact, Pipe and Connection), but we used just beams and cut-off bars.

Beam

The beam type refers to the conventional beam element with six degrees of freedom at each node: three translations and three rotations. The beam carries axial force, shear force, bending moment and torque.

The element is a straight line between the two nodes to which it is connected, but may deform into a cubic shape. The beam may be used as a thin beam

where all out of plane deformation is due to bending or as a thick beam where deformation is due to both bending and shear.

Cut-off bar

The cut-off bar element is a truss element that has predefined tension and compression load limits. If the axial load in the bar exceeds the set limits, the bar fails. This type of element is mostly used as a gap element. We used this elements to represent the cables.

2) ***Links*** are similar to beam elements except that they define how the displacements/rotations of one node are related to the displacements/rotations of another one. This relation is enforced via additional equations in the stiffness matrix, known as Lagrange equations.

Rigid Link

The Rigid Link provides an infinitely stiff connection between two nodes. However, the rigid link also provides constraints on the nodal rotation such that there is no relative rotation between the connected nodes. It is used to connected the cross beams with the deck.

3) ***Plate*** is a generic name for a group of two-dimensional surface elements. The surface elements (always referred to as "plates" in Straus7) include the three and six node triangular elements, and four, eight and nine node quadrilateral elements like shown in figure 1.7.

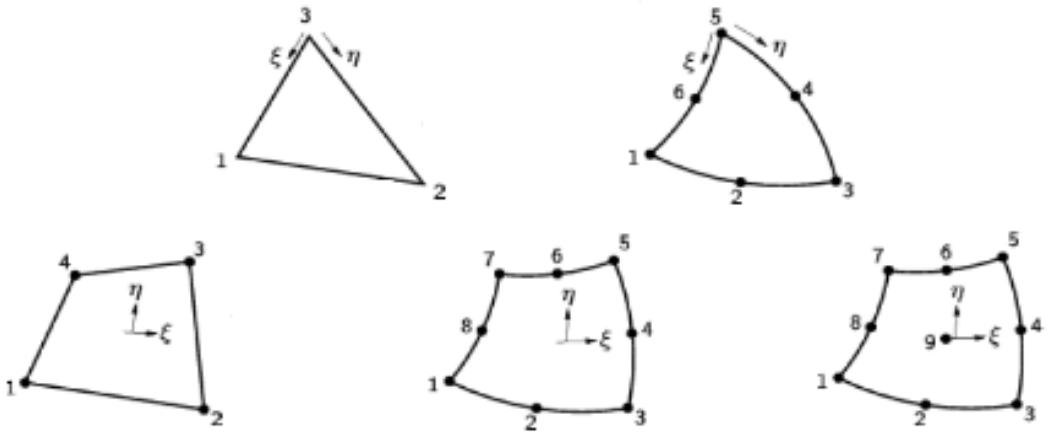

Figure1.7. The ISO3, ISO6 triangles, ISO4, ISO8 and ISO9 quadrilaters.

These elements can be used for plane stress and plane strain analysis, asymmetric solid problems, plate and shell analysis, as shear panels, 3D membranes and for heat flow analysis. The table 1.1 shows the way in which plate elements may be used in Straus7.

	2D Plane Stress	2D Plane Strain	Axisymmetric	ThinPlate/ Shell	ThickPlate /Shell	Shear Panel	3D Membrane	Heat Transfer
Tri3	✓	✓	✓	✓			✓	✓
Quad4	✓	✓	✓	✓		✓	✓	✓
Tri6	✓	✓	✓	✓	✓		✓	✓
Quad8	✓	✓	✓	✓	✓		✓	✓
Quad9	✓	✓	✓	✓	✓		✓	✓

Table1.1 elements related to the case of study

The deck of the bridge is made by shell elements:

Plate/Shell

The plate/shell element is the most general type of plate element in that it is a three-dimensional membrane and bending element. It is the only plate element that permits out of plane displacements associated with bending behaviour. This includes the analysis of flat plates and general three-dimensional shells. The default freedom condition should be set free in all directions. This element is the most commonly used plate element. Typical applications are shown in figure

2.5.2 Type of Analysis

Straus7 offers two solver technologies: a skyline solver and a sparse solver. The skyline solver can be very efficient for small models, but its performance is greatly affected by the bandwidth of the matrix. The Straus7 sparse solver is a high performance option that is useful for large models. Sparse solvers allow very fast solution of large systems of equations by exploiting the so-called sparsity of the matrix. A matrix is sparse if the number of non-zero entries is small compared with the total number of entries in the matrix.

The analysis that the software provides can be divided in three principal groups:

1. ***Static Analysis***
   Linear Static
   Nonlinear Static
   Linear Buckling

2. ***Dynamic Analysis***
   Natural Frequency
   Harmonic Response
   Spectral Response
   Linear Transient
   Nonlinear Transient

We are going to introduce just the Linear Static and the Natural Frequency analysis because these are the one we used in the work.

Linear Static

The linear static solver is the most widely used among the various solvers available. A linear static solution by this solver is obtained assuming that the structure's behaviour is linear and the loading is static.

For the response of a structure to be linear, the mechanical behaviour of all materials in the model must follow Hooke's law; i.e., element forces are linearly proportional to element deformation and when the loading is removed, the material returns to its original shape. In addition, the deformation must be so small that the deformed geometry is undistinguishable from the original one. Because of these two assumptions, solutions can be arbitrarily combined to consider more complex loading conditions. A load is regarded as static if its magnitude and direction do not change with time. Structures under static loading conditions are analysed with the inertial and damping properties ignored.

The Linear Static Solver performs the following steps:

1) Calculates and assembles element stiffness matrices, equivalent element force vectors and external nodal force vectors. Constraints are also assembled in this

process. At the end of this assembly procedure, the following linear system of equilibrium equations is formed:

$$[K]\{d\} = \{P\}$$

where

$[K]$ is the global stiffness matrix;

$\{d\}$ is the unknown nodal displacement vector(s);

$\{P\}$ is the global nodal load vector(s).

2) Solves the equations of equilibrium for the unknown nodal displacements.

3) Calculates element strains, stresses, stress resultants and strain energy densities etc. as requested.

Natural Frequency

The natural frequency solver is used to calculate the natural frequencies (or free vibration frequencies) and corresponding vibration modes of an undamped structure. The natural frequency analysis problem, is formulated as the following eigenvalue problem:

$$[K]\{x\} = \omega^2 [M]\{x\}$$

where

$[K]$ is the global stiffness matrix;

$[M]$ is the global mass matrix;

$\{x\}$ is the vibration mode vector ;

ω is the natural (circular) frequency (radians/sec).

The Natural Frequency Solver performs the following steps:

1) Calculates and assembles the element stiffness and mass matrices to form the global stiffness and mass matrices. In the stiffness calculation, material temperature dependency is considered. Either a consistent or lumped mass matrix can be used according to the solver option setting . Constraints are assembled in this process. If the initial file is from a nonlinear solution, the stiffness and mass matrices calculation will be based on the current material status and geometry. More specifically, the current

material modulus values will be used for nonlinear elastic material. For plastic material, the initial modulus is used. The current geometry is used if geometric nonlinearity is considered in the initial solution.

2) Checks the mass matrix. If all diagonal entries are zero, the solution stops.
3) Solves the eigenvalue problem to get the natural frequencies of the structures.

2.6 Case of study (description of the Footbridge)

The footbridge we are analysing in this work, was designed by the engineer Leopoldo Gasparetto Stori and serves as a connection of the two side of a park, over crossing the new della Costituzione road replacing a stretch of the Emilia main road in the Pedagna neighbourhood in Imola. Imola is a little town in the north-central Italy.

The footbridge has a total length of 51 m between abutments and it is a two span bridge. The bridge main span is 47 m and the lane width is 3,5 m. The footbridge consists of a Y-shaped inclined tower, six cables stays (3 on each side of the deck) connected in a fan-type configuration and a deck made of steel tubes connected each other and welded supported a concrete slab of 12 cm thickness.. The deck has a skew angle of 3,6 ° and is comprised of 27 steel tubes, which have a diameter of 193 mm and a thickness of 8 mm, what to improve the torsional rigidity, to resist to transverse bending and to transfer load between the stay cable anchorage, there is also a concrete slab with a total thickness of 12 cm cooperating with the tubes. The footbridge is anchored at the end and it is supported along its length by three couples of cables. The cables are anchored to an inclined pylon made of metal welded sheets which enclose the reinforced concrete core inside.

All along the bridge there are glass panels which have an aesthetic function and protect people from the wind.

In the figure 1.9, a schematic drawing of the footbridge is shown.

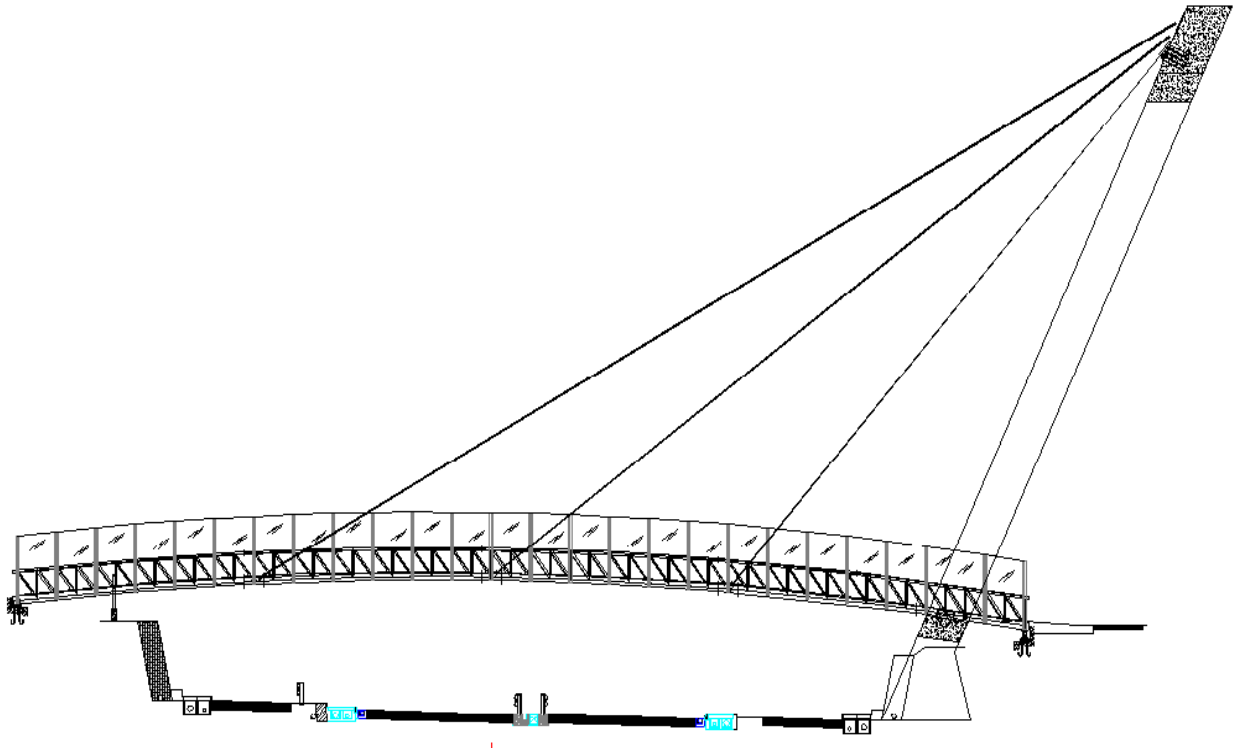

Figure1.8. The footbridge draw

2.7 The FEM model of the Footbridge

In this study, all the investigations were conducted before the public opening of the bridge. During the test load deflections, acceleration and stresses were measured.
Theoretical results compared with the measured data provide useful information about the initial state of the bridge and they could be used for a comparison with later studies and investigations. It is an important instrument to check the state of the bridge along its life.

The model, as we saw in the 1.5 paragraph, is created by a software program for the structural analysis called STRAUS7.
In defining the FEM model, both the geometric features and the material properties were taken from written design documentation and drawings.
The **deck** and the **lateral trusses** of the bridge are modelled using beam type elements with a circular cross-section, connected at the nodes. It is decided to use this type of

element that can transfer axial and shear forces and moments, because the tubes are welded each other. Actually the tubes forming the two lateral trusses of the bridge, are almost completely subjected to compression forces. Instead the transversal tubes connecting the two sides and creating the base for the deck have to carry also moments and shear forces, due to the lack of diagonal elements.

The total thickness of the deck is 12 cm, but the concrete slab is just 7 cm modelled with 2D elements, I mean shell. A shell is a three dimensional body with one dimension much smaller than the other two and the curvature of the shell mid-surface in the current configuration is non-zero. This element is studied with the Reissner, Mindlin theory. The presence of a corrugated sheet cooperating with the concrete slab suggested us to use the shell element that has a flexural stiffness. We have to find the right thickness of the deck considering an homogeneous material, thus we used the following approach:

1. First of all it the total area of the deck is calculated,

$$A = l \cdot b = 51 \cdot 3 = 153 \quad \left[m^2 \right] \tag{1}$$

where l is the total length and b is the transversal dimension of the bridge.

2. Then the homogenized volume is obtained:

$$V_{TOT} = (l \cdot b \cdot s_c) + \frac{E_s}{E_c} \cdot \left[n \cdot \pi \left(\frac{\phi}{2} \right)^2 \cdot l_b \right] + (l \cdot b \cdot s_l) =$$

$$= (51 \cdot 3 \cdot 0,07) + 7 \left[20 \cdot 3,1415 \cdot \left(\frac{0,006}{2} \right)^2 \cdot 51 \right] + (51 \cdot 3 \cdot 0,01) = 12,4 \quad \left[m^3 \right] \tag{2}$$

where s_l is the sheet metal thickness, ϕ is the diameter of the bar and n is the number of bars.

3. And finally the thickness of the equivalent homogeneous shell is given by the following expression:

$$s_{tot} = \frac{V_{tot}}{A} = \frac{12,4}{153} = 0,08 \quad [m] \quad = \quad 80mm$$

(3)

To find the bending thickness we have to consider the concrete cracking. There are two main cases:

when the section of the bridge is completely in compression the moment of inertia is J_{TOT}, instead when the slab is cracked (where some of the fibres are in tension) the value of the moment of inertia is usually considered $\frac{1}{3}\ J_{TOT}$. In general is suggested to use a middle value between the two cases, therefore we have considered a value equal to $\frac{2}{3}J_{TOT}$.

The connection between the transversal tubes and the deck is made by rigid link. It provides an infinitely stiff connection between two nodes. However, the rigid link also provides constraints on the nodal rotation such that there is no relative rotation between the connected nodes.

The inclined ***pylon*** consists of several metal welded panels, whose thickness is 4,5 cm that contains a reinforced concrete core. In order to model this pylon, it is divided in four parts according to the amount of steel bar inside. Considering that it is really high and slender, it could be modelled by four beam elements having different dimensions.
The material should be homogeneous, therefore the geometrical proprieties of the beams cross section are evaluated. Two different approaches are analyzed to obtain the values of moments of inertia and of area:

1. it is simply considered the sum of the contributions of the two different materials;
2. it is obtained the equivalent cross section having both the area and the moment of inertia in the main direction equal to the combined contributions of concrete, metal shells and bars.

Pylon piece 0

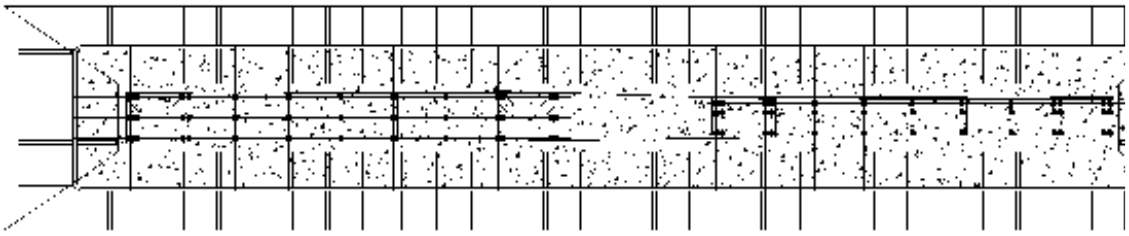

Figure1.9. The cross section of the beam at the bottom of the pylon

b	width	3500	*mm*
h	height	600	*mm*
s_l	thickness	12	*mm*

Equivalent area

$A_s = \frac{E_s}{E_c} \cdot n \cdot \pi \left(\frac{\phi}{2} \right)^2$	steel bars	215533,71	mm^2
$A_l = \frac{E_s}{E_c} \cdot s_l \cdot b$	steel sheets	688800	mm^2
$A_c = h \cdot b$	concrete	2100000	mm^2
$A_{tot} = A_s + A_c + A_l$	total	**3004333,71**	mm^2

Moment of inertia around the longitudinal axis X J_x

$J_{xs} = \sum_i A_{si} \cdot d_i^{\,2}$	steel bars	1038154037	mm^4
$J_{xl} = 2 \cdot A_l^{\,i} \cdot (h + s/2$	steel sheets	27528984000	mm^4
$J_{xc} = \frac{bh^3}{12}$	concrete	63000000000	mm^4
$J_{xtot} = J_{xs} + J_{xl} + J_{xc}$	total	**91567138037**	mm^4
	heq	604,76	*mm*
	beq	4967,78	*mm*
J_z		**6,17861E+12**	mm^4

Pylon piece 1

We decided to use a simple proportion to deduce the dimension of this second part.

B	width	2400	*mm*
H	height	600	*mm*
S	thickness	12	*mm*

by proportion

Beq		3480,7	*mm*
Heq		600,1	*mm*

Original dimensions

B	width	2000	*mm*
H	Height	600	*mm*
S	thickness	12	*mm*

Equivalent area

$A_s = \frac{E_s}{E_c} \cdot n \cdot \pi \left(\frac{\phi}{2} \right)^2$	steel bars	103775,49	mm^2
$A_l = \frac{E_s}{E_c} \cdot s_l \cdot b$	steel sheets	436800	mm^2
$A_c = h \cdot b$	concrete	1200000	mm^2
$A_{tot} = A_s + A_c + A_l$	total	1740575,49	mm^2

Moment of inertia around the longitudinal axis X J_x

$J_{xs} = \sum_i A_{si} \cdot d_i^{\,2}$	steel bars	499851944	mm^4
$J_{xl} = 2 \cdot A_l^{\,i} \cdot (h + s/2)$	steel sheets	1,57E+10	mm^4
$J_{xc} = \frac{bh^3}{12}$	concrete	3,6E+10	mm^4
$J_{xtot} = J_{xs} + J_{xl} + J_{xc}$	total	**5,22E+10**	mm^4

heq		**600,1**	*mm*
beq		**2900,6**	*mm*

J_z		**1,2203E+12**	mm^4

Pylon piece 2

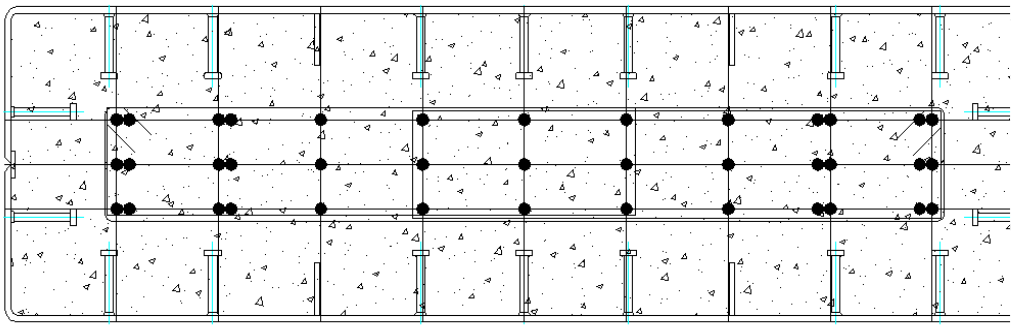

Figure1.10. The cross-section of the second beam

b	width	600	*mm*
h	height	2000	*mm*
s	thickness	12	*mm*

Equivalent area

$A_s = \frac{E_s}{E_c} \cdot n \cdot \pi \left(\frac{\phi}{2}\right)^2$	steel bars	103775,49	mm^2
$A_l = \frac{E_s}{E_c} \cdot s_l \cdot b$	steel sheets	436800	mm^2
$A_c = h \cdot b$	concrete	1200000	mm^2
$A_{tot} = A_s + A_c + A_l$	total	**1740575,5**	mm^2

Moment of inertia around the longitudinal axis X J_x

$J_{xs} = \sum_i A_{si} \cdot d_i^{\,2}$	steel bars	3,1572E+10	mm^4
$J_{xl} = 2 \cdot A_l^{\,i} \cdot (h + s/2)$	steel sheets	4,4206E+11	mm^4
$J_{xc} = \frac{bh^3}{12}$	concrete	4E+11	mm^4
$J_{xtot} = J_{xs} + J_{xl} + J_{xc}$	total	**8,7363E+11**	mm^4

beq	**2454,2**	*mm*
heq	**709,2**	*mm*
J_z	7,296E+10	mm^4

Using the first method we reach the following results

concrete area	1740575,49	mm^2
$J_{xc} = \frac{bh^3}{12}$	5,2231E+10	mm^4
$J_{xc} = \frac{hb^3}{12}$	8,7363E+11	mm^4

Pylon piece 3

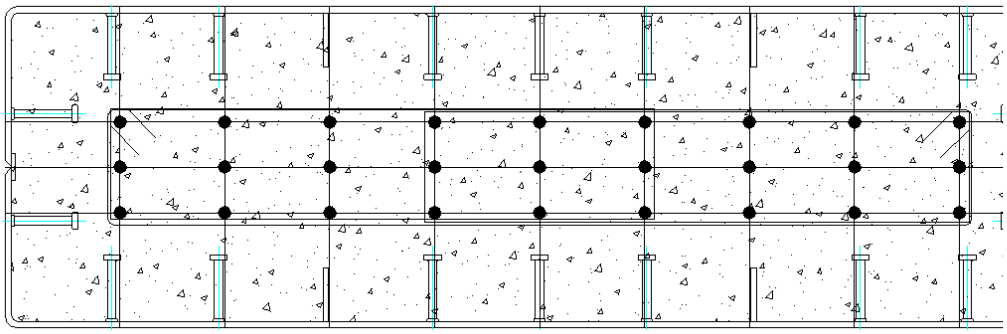

Figure1.11. The cross-section of the third beam

b	width	600	*mm*
h	height	2000	*mm*
s	thickness	12	*mm*

Equivalent area

$A_s = \frac{E_s}{E_c} \cdot n \cdot \pi \left(\frac{\phi}{2}\right)^2$	steel bars	71844,57	mm^2
$A_l = \frac{E_s}{E_c} \cdot s_l \cdot b$	steel sheets	436800	mm^2
$A_c = h \cdot b$	concrete	1200000	mm^2

$A_{tot} = A_s + A_c + A_l$	total	1708644,57	mm^2

Moment of inertia around the longitudinal axis X J_x

$J_{xs} = \sum_i A_{si} \cdot d_i^{\,2}$	steel bars	346051346	mm^4
$J_{xl} = 2 \cdot A_l^{\,i} \cdot (h + s/2)$	steel sheets	1,5731E+10	mm^4
$J_{xc} = \frac{bh^3}{12}$	concrete	3,6E+10	mm^4
$J_{xtot} = J_{xs} + J_{xl} + J_{xc}$	total	**5,2077E+10**	mm^4
heq		**604,8**	*mm*
beq		**2825,3**	*mm*
J_z		**1,1366E+12**	mm^4

Using the first method we reach the following results:

Concrete area	1708644,6	mm^2
$J_{xc} = \frac{bh^3}{12}$	5,2077E+10	mm^4
$J_{xc} = \frac{hb^3}{12}$	4,7934E+11	mm^4

Pylon piece 4

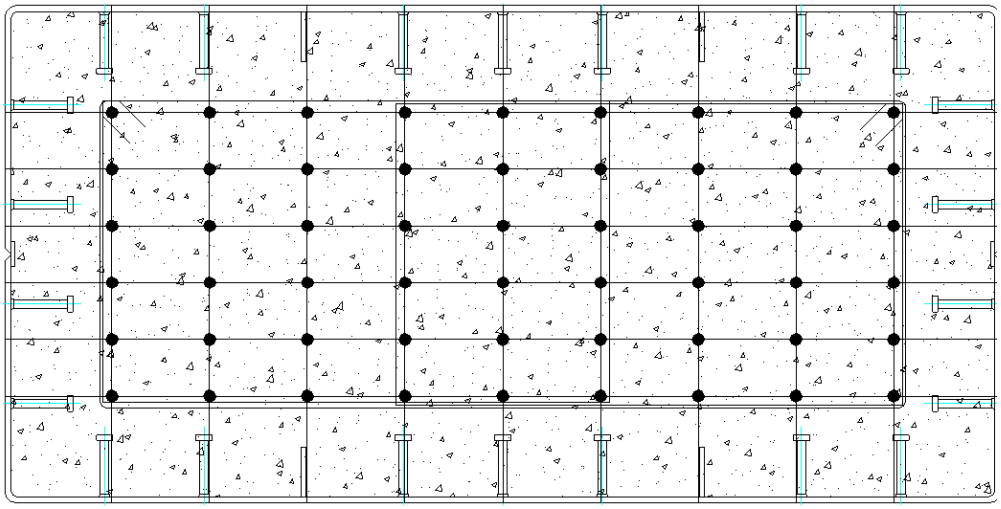

Figure1.12. The cross-section of the top beam

b	width	2000	*mm*
h	height	1000	*mm*
s	thickness	12	*mm*

Equivalent area

$A_s = \frac{E_s}{E_c} \cdot n \cdot \pi \left(\frac{\phi}{2}\right)^2$	steel bars	143689,14	mm^2
$A_l = \frac{E_s}{E_c} \cdot s_l \cdot b$	steel sheets	504000	mm^2
$A_c = h \cdot b$	concrete	2000000	mm^2
$A_{tot} = A_s + A_c + A_l$	total	2647689,14	mm^2

Moment of inertia around the longitudinal axis X

$J_{xs} = \sum_i A_{si} \cdot d_i^{\,2}$	steel bars	5446536852	mm^4
$J_{xl} = 2 \cdot A_l^{\,i} \cdot (h + s/2)$	steel sheets	1,3646E+10	mm^4
$J_{xc} = \frac{bh^3}{12}$	concrete	1,6667E+11	mm^4
$J_{xtot} = J_{xs} + J_{xl} + J_{xc}$	total	**1,8576E+11**	mm^4

heq	**917,6**	*mm*
beq	**2885,6**	*mm*
J_z	**1,8372E+12**	mm^4

Using the first method we reach the following results:

Equivalent area	2647689,14	mm^2
$J_{xc} = \frac{bh^3}{12}$	1,8576E+11	mm^4
$J_{zc} = \frac{hb^3}{12}$	7,7192E+11	mm^4

Pylon transversal beam

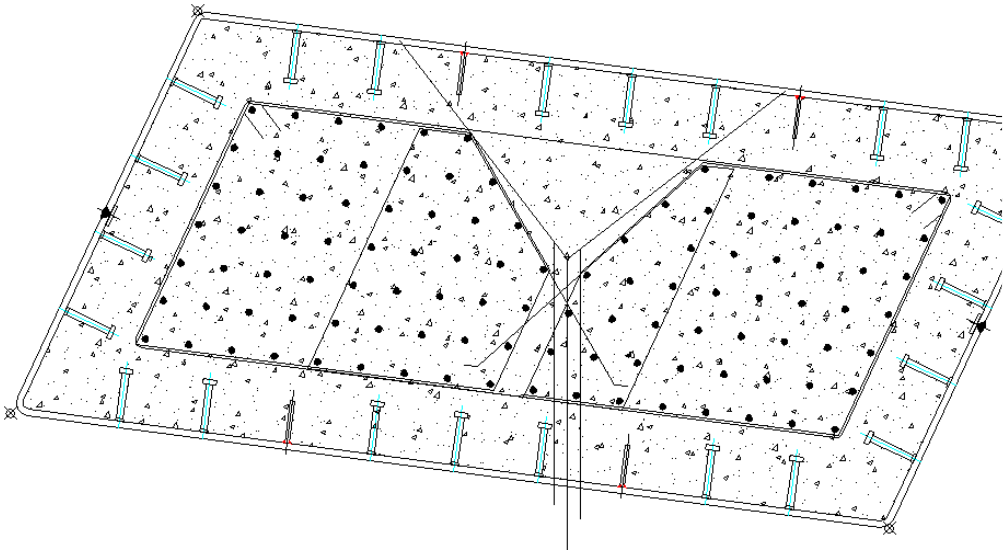

Figure1.13. The cross section of the transversal beam

b	width	12	*mm*
h	height	1000	*mm*
s	thickness	2060	*mm*

equivalent area

$A_s = \frac{E_s}{E_c} \cdot n \cdot \pi \left(\frac{\phi}{2} \right)^2$	steel bars	167484,646	mm^2
$A_l = \frac{E_s}{E_c} \cdot s_l \cdot b$	steel sheets	514080	mm^2
$A_c = h \cdot b$	concrete	2060000	mm^2
$A_{tot} = A_s + A_c + A_l$	total	**2741564,646**	mm^2

Moment of inertia around the longitudinal axis X

$J_{xs} = \sum_i A_{si} \cdot d_i^{\,2}$	steel bars	6134541735	mm^4
$J_{xl} = 2 \cdot A_l^{\,i} \cdot (h + s/2)^2$	steel sheets	88608938880	mm^4
$J_{xc} = \frac{bh^3}{12}$	concrete	1,71667E+11	mm^4
$J_{xtot} = J_{xs} + J_{xl} + J_{xc}$	total	**2,6641E+11**	mm^4
heq		**1079,9**	*mm*
beq		**2538,8**	*mm*
J_z		**1,47259E+12**	mm^4

Using the first method we reach the following results:

concrete area	2741564,646	mm^2
$J_{xc} = \frac{bh^3}{12}$	2,6641E+11	mm^4
$J_{zc} = \frac{hb^3}{12}$	8,33743E+11	mm^4

The ***connection*** between the bridge and the deck is provided by two hinges that are realized using a beam with a high stiffness equal to $1 \cdot 10^6\ MPa$ and end rotations released.

The other ***supports*** are modelled as is shown in the design draws and as it explained in the following figure(1.14).

Figure1.14. The visualisation and disposition of the supports.

The symbol U indicates a roller that has only a single translational degree of freedom, while the symbol M indicates a roller which has two translational degrees of freedom and only the degree of freedom in the vertical direction is blocked. Finally the letter F represents a fixed point/support. The units of measure are in mm.

The ***glass panels*** distributed all along the footbridge don't have a structural function and hence have been modelled as translational masses.

The weight of the panel was divided in two points, one at the height of the hand rail and the other one at the bottom of the deck, according to the following calculation and considering the area of influence for each part.

We are going to show the calculus:

Glass sheet

h_1	length of the top part	1695 (mm)
h_2	length of the bottom part	1305 (mm)
s_g	thickness of the panel	10 (mm)
γ_g	Specific weight of glass	2,7e-9 (T/mm^3)
Weight of the first panel	$W_1 = h_1 \cdot s_g \cdot \gamma_g \cdot \Delta l = 46,62$	Kg
Weight of the second panel	$W_2 = h_2 \cdot s_g \cdot \gamma_g \cdot \Delta l = 31,32$	Kg

Where Δl is the wide of the panel and corresponds also to the distance between the two transversal beams of the deck equal to 2000 mm. This is just the weight of the internal glass panel, but we have to sum the contribution of the metal frame to each panel. In the extreme part the value of weight is the half part because the influenced area is halved.

The structure is a cable-stayed bridge for its strands that support the deck, so we have to decide also how to model the ***cables***.
The cable is an element with geometrical non linear behaviour; it does not react in compression and its stiffness depends both from the tension and the curvature of the cable itself. The Dishinger module governs its behaviour and is expresses as follow (equation 4).

$$d\sigma = Ed\varepsilon = \frac{E}{1+\frac{\gamma^2 l^2 E}{12\sigma^3}} \cdot \frac{dl}{l} \tag{4}$$

where

$d\sigma$ is the increase of tension in the cable;

$d\varepsilon$ is the increase of deformation in the cable;

E is the elastic module of the material;

γ is the specific weight of the material;

l is the initial length of the cable;

σ is the tension in the cable;

dl is the increasing length of the cable.

Anyway as a first approximation, for the static validation and to find the natural frequency we need a linear model therefore the cables are modelled by ***cut-off elements***. They are similar to the trusses, but have predefined tension and compression load limits. If the axial load in the beam exceeds the set limits, the bar fails. This type of element is mostly used as a gap element. The cutoff bar can be used as the following gap elements:

1. Tension Only: a beam element that is automatically removed from the model if it ever goes into compression or if the tension reaches a predetermined cut-off value.
2. Compression Only: a beam element that is automatically removed from the model if it ever goes into tension or if the compression reaches a predetermined cut-off value.
3. Tension-Compression: a beam element that resists both tension and compression, but only to predetermine (compression and tension) cut-off values.

In addition to the cut-off value, the elements have an option to specify what happens to the bar if its axial force exceeds the cut-off value. Two options are possible:

Brittle

When the axial load in the bar exceeds one of the limits, the bar fails completely and contributes no further stiffness to the model. The bar is removed from the model.

Ductile

If the axial load in the bar exceeds the limit, the bar becomes plastic and yields whilst continuing to carry the maximum permissible load. The load cannot however exceed the set limit.

The actual breaking force that is used to stop the tension is 759,6 KN and the elastic module is the one of the steel and it is equal to 2,06 *10^5 MPa.

In the last chapter we are going to introduce the non linear behaviour of the cable using a diagram stress versus strain and the Dischinger elastic module.

In the following page the FEM model of the bridge is reported, (figure 1.15).

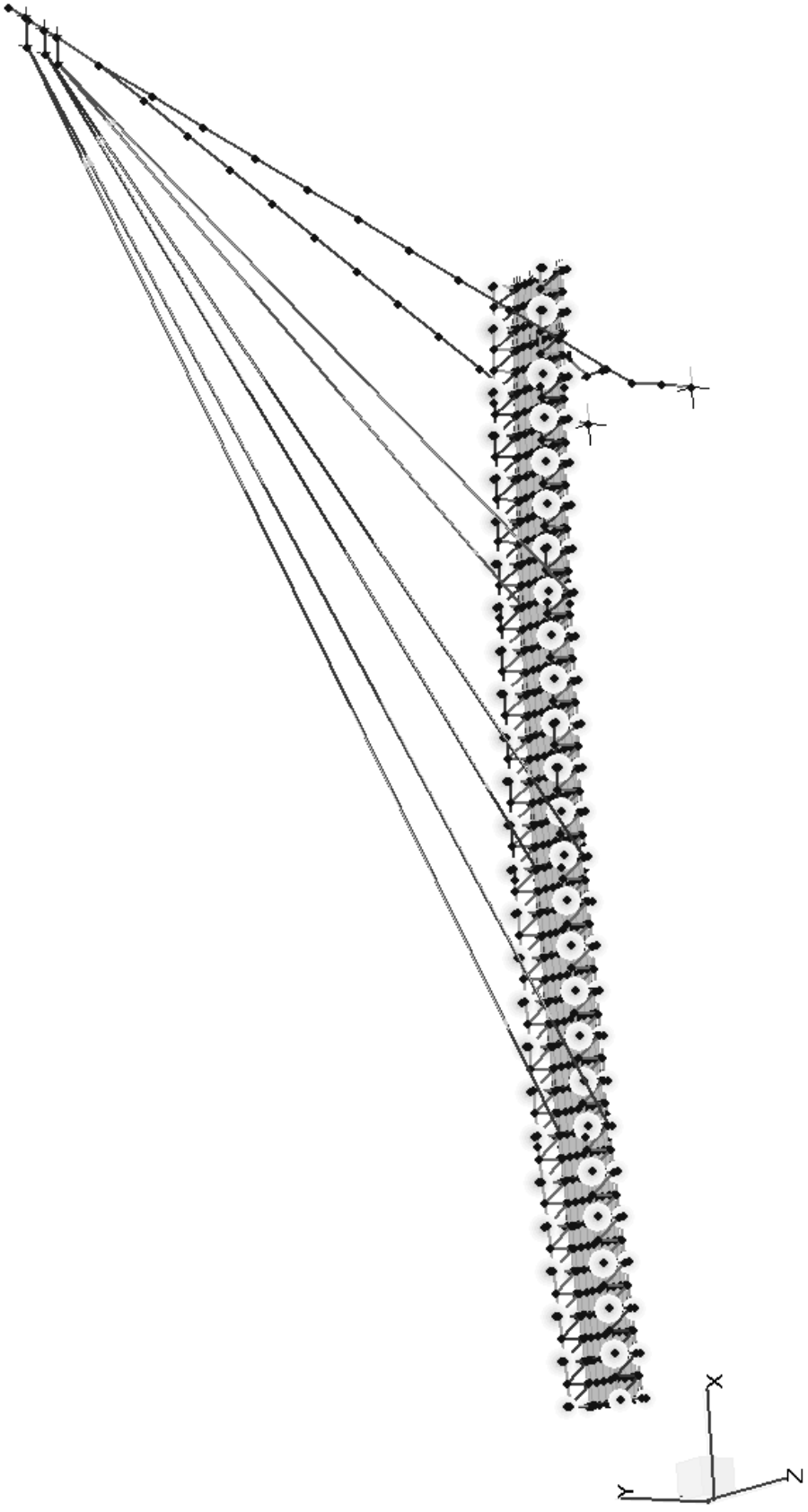

Figure1.15. The FEM model of the bridge.

Chapter 2

2.1 Introduction

With the term System Identification we indicate the complex process of identifying a mathematical model of a system , model that represent the dynamic characteristics and behaviour of it, (e.g. natural frequencies, damping ratios, mode shapes) of structures. In order to obtain the dynamic proprieties of a structure and study its behaviour under a generic load condition, a mathematical model is necessary. This describes the relations between forces, displacements, velocities, accelerations and flexures of the system.

The classic method to study the relation of the output *x(t)* of a system with a generic external force *f(t)* is to solve the differential dynamic equations with the Integral method. However the most part of the problems is too elaborated it's not easy to find the output using the. Thus, the frequency response approach is commonly used. This last approach, that is used by the identification techniques determines the dynamic proprieties of the system through the Frequency Response Function FRF. A frequency response function (FRF) is a transfer function, expressed in the frequency domain. Frequency response functions are complex functions, with real and imaginary components. They may also be represented in terms of magnitude and phase. A frequency response function can be formed from either measured data or analytical functions.

A frequency response function expresses the structural response to an applied force as a function of frequency. The response may be given in terms of displacement, velocity, or acceleration. This kind of functions is used in vibration analysis and modal testing and it could be used either if the behaviour of the structures is linear or non-linear [Sabia, 1997]. The FRF can be obtained directly for a harmonic force or, in case of different excitation, it is determined by the signal processing. It uses the autocorrelation and cross-correlation function applied to output and input signals.

In this chapter we are going to review the bases of the Dynamic of Structures focusing on the representation of mechanical system through state variables.

2.2 Dynamic system

A system is defined dynamic when the forces change with the time and cause significant inertial force. To study this case, we can adopt a determinist, stochastic or random approach depending on the kind of forces involved. It is called "deterministic approach" if we know the evolution of the force with the time, otherwise the process is un-deterministic, that is the most frequent case.

In addition, we need to define the kind of problem we are interested in. It can be directed and inverse.

1. In a ***directed problem,*** the external force and the analytical model are known and they are used to obtain the response of the dynamic system to the external excitation.
2. In an ***inverse problem,*** the output of the system is known. Moreover this could be subdivided in other three groups:
   - ✓ *Design problem*: the external force is known and the model of the system is created referring to limitation and information about the output.
   - ✓ *Control problem*: knowing the geometrical proprieties and the output of the system, the external excitation is determined.
   - ✓ *Identification problem*: knowing the output and the force, the model of the system is determined.

The classical definition of the identification problem could be extended also to the cases with external force unknown, and this is the type of analysis we are going to describe in this dissertation. This kind of problem is called output only system identification.

The theory of linear SDOF and MDOF systems is the foundation of Experimental Modal Analysis.

2.2.1 Single degree of freedom systems (SDOF);

A dynamic Single Degree of Freedom (SDOF) system is shown in figure 2.1. The spring represents the stiffness of the system and the viscous damper is included to model the dissipation of energy. If the restoring force from the spring is proportional to the deflection and the viscous dissipative force is proportional to the velocity, such a SDOF system is linear (i.e. additive and homogenous). A mass m [kg] which can move in direction of x-axis is connected to a fixed base by a spring described by its stiffness coefficient k [N/m] and a dashpot (viscous damper) with the damping coefficient c [N/(m/s)]. The mass may be excited by a force F(t) that varies with time and the objective of analysis is the prediction of the response of the mass to excitation, its behaviour in the period after the excitation ceased (free vibration) or the effect of frequency content of excitation.

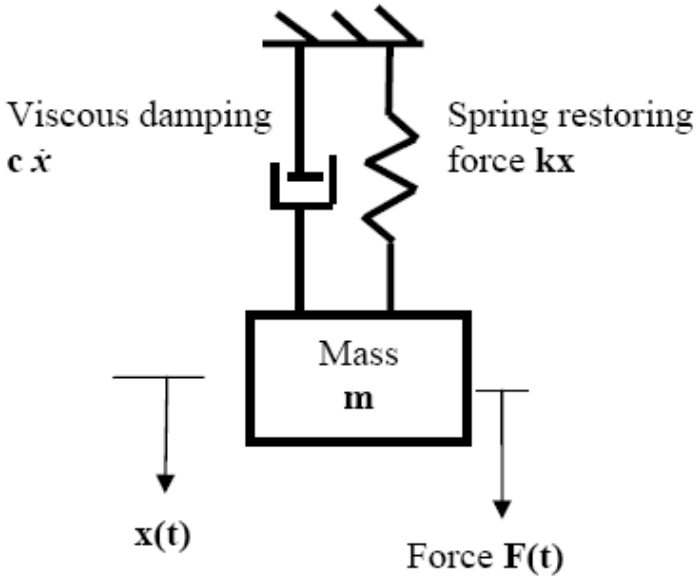

Figure1.16. SDOF system representation

Indicating with $x(t)$ the temporal history of the displacement, the following 2^{nd} order equation, called equation of motion, is obtained:

$$m\ddot{x} + c\dot{x} + kx = F(t) \tag{5}$$

Let's considered the homogeneous equation (free vibrations) without the external force $F(t) = 0$.

$$m\ddot{x} + c\dot{x} + kx = 0 \tag{6}$$

The chosen solution has the following expression:

$$x(t) = Xe^{st} \tag{7}$$

and, substituting it in the dynamic equation, after some mathematical passages is obtained:

$$s^2 + 2\zeta\omega_n s + \omega_n^2 = 0 \tag{8}$$

where ω_n is the natural frequency of the system:

$$\omega_n = \sqrt{\frac{k}{m}} \tag{9}$$

and ζ is the damping ratio:

$$\zeta = \frac{c}{2m\omega_n} = \frac{c}{c_0} \tag{10}$$

where c_0 is the critical damping coefficient.

Solving the equation in the variable s, the two complex solutions are determined:

$$s_{1,2} = -\omega_n\varsigma \pm i\omega_n\sqrt{1-\varsigma^2} = -\omega_n\varsigma \pm i\omega_d \tag{11}$$

The solution of the dynamic system is:

$$x(t) = Xe^{-\omega_n \varsigma t} e^{i\omega_d t} \tag{12}$$

and it defines the single mode of the system. The first term $e^{-\omega_n \varsigma t}$ corrispond to the exponetially decay part and the second to the periodic component. The complex frequency consists of two parts: the imaginary or oscillatory part with frequency $\omega_n \sqrt{1-\varsigma^2}$ and the real one with frequency ω_n .

The displacement of an underdamped system would appear like the figure 2.2.

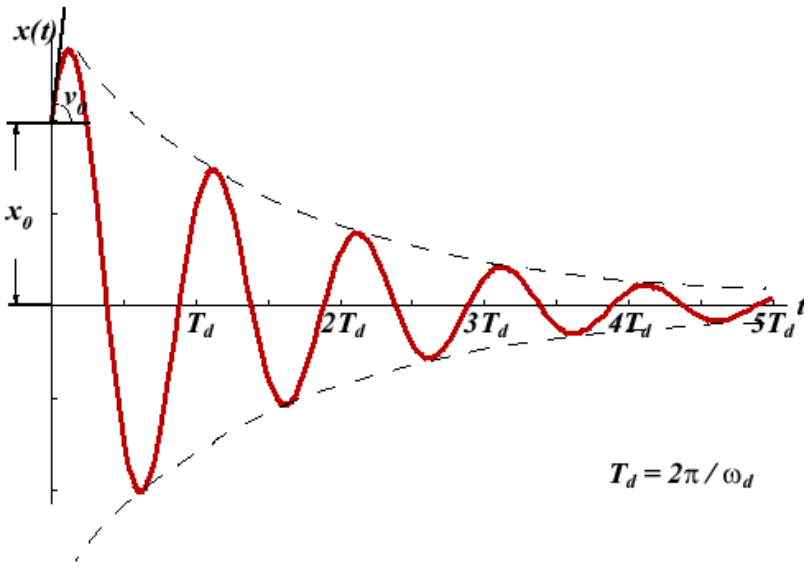

Figure1.17. displacement plot of a SDOF underdamped system

where $T_d = \dfrac{2\pi}{\omega_d}$ is the period f the dumped vibration.

2.2.2 Multi degree of freedom systems (MDOF)

Equation of motion

The behaviour of a dynamic system that is linear and with *N* degrees of freedom is governed by the following equations of motion:

$$\underset{\sim}{\mathbf{M}}\ddot{\mathbf{v}}(t)+\underset{\sim}{\mathbf{C}}\dot{\mathbf{v}}(t)+\underset{\sim}{\mathbf{K}}\mathbf{v}(t)=\mathbf{f}(t)$$

(13)

where $\mathbf{v}(t)$, $\dot{\mathbf{v}}(t)$, $\ddot{\mathbf{v}}(t)$ are, respectively, the displacement, the velocity and the acceleration vectors, related to the degrees of freedom of the system

$\underset{\sim}{\mathbf{M}}$, $\underset{\sim}{\mathbf{C}}$ and $\underset{\sim}{\mathbf{K}}$ are the mass, the damping and the stiffness matrices, respectively. Each one of dimension N x N. Finally, $\mathbf{f}(t)$ is the vector of the external forces and its dimension is N.

The natural frequencies, the damping ratios and the mode shape are obtained through the homogeneous equation:

$$\underset{\sim}{\mathbf{M}}\ddot{\mathbf{v}}(t)+\underset{\sim}{\mathbf{C}}\dot{\mathbf{v}}(t)+\underset{\sim}{\mathbf{K}}\mathbf{v}(t)=0$$

(14) Supposing the solution of the previous equation is a harmonic function:

$$\mathbf{v}=\boldsymbol{\varphi}e^{\lambda t}$$

(15)

and substituting $\mathbf{v}$ in the homogeneous equation, the associated eigenvalue problem can be expressed as:

$$\left(\underset{\sim}{\mathbf{M}}\lambda^2+\underset{\sim}{\mathbf{C}}\lambda+\underset{\sim}{\mathbf{K}}\right)\boldsymbol{\varphi}=\mathbf{0}$$

(16)

Assuming that the structure has all the rigid –body modes constrained and there are no repeated eigenvalues, the solution of the equation (12) provides N eigenvalues and N eigenvectors that are complex variables. The eigenvalues determined solving the equations above, are usually written as follow [Ewins, 2000]:

$$\lambda_j=-\omega_j\zeta_j+i\omega\sqrt{1-\zeta_j^{\,2}}$$

(17)

where ω_j is j-th frequency for an un-damped system and ζj is the damping ratio respectively.

2.2.3 Equation of motion in a state space form

Another form to represent the equations of motion of a dynamic system is through a state space realization such as:

$$\dot{\mathbf{x}}(t) = \underset{\sim}{\mathbf{A}}_c \mathbf{x}(t) + \underset{\sim}{\mathbf{B}}_c \mathbf{u}(t) \tag{18}$$

which is obtained writing the classical second order equation of motion in the state space form, using the response vector and the system matrices in the state form

$$\mathbf{x}(t) = \begin{bmatrix} \mathbf{v}(t) \\ \dot{\mathbf{v}}(t) \end{bmatrix} \tag{19}$$

$$\underset{\sim}{\mathbf{A}}_c = \begin{bmatrix} \underset{\sim}{\mathbf{0}} & \underset{\sim}{\mathbf{I}} \\ -\underset{\sim}{\mathbf{M}}^{-1}\underset{\sim}{\mathbf{K}} & -\underset{\sim}{\mathbf{M}}^{-1}\underset{\sim}{\mathbf{C}} \end{bmatrix} \tag{20}$$

where $\mathbf{x}(t)$ is the state space vector containing the displacement and velocity vectors and $\underset{\sim}{\mathbf{A}}_c$ is a matrix containing the system's mass, damping and stiffness matrices. In the equations above $\underset{\sim}{\mathbf{0}}$, $\in R^{N*N}$, is the null matrix and $\underset{\sim}{\mathbf{I}}$, $\in R^{N*N}$ is the identity matrix. The eigenvalue problem associated with the equations above is now in term of an asymmetric matrix:

$$\underset{\sim}{\mathbf{B}}_c = \begin{bmatrix} \underset{\sim}{\mathbf{0}} \\ \underset{\sim}{\mathbf{M}}^{-1} \end{bmatrix} \tag{21}$$

$$\mathbf{u}(t) = \begin{bmatrix} \mathbf{0} \\ \mathbf{f}(t) \end{bmatrix} \tag{22}$$

The system consists of 2*N* first order differential equations. The corresponding equations of motion for free vibration of a linear system can be written as follow:

$$\dot{\mathbf{x}}(t) = \underset{\sim}{\mathbf{A}}_c \mathbf{x}(t) \tag{23}$$

just setting equal to zero the vector of the external force $\mathbf{u}(t)$.

A harmonic solution is assumed in order to solve the problem:

$$\mathbf{x}(t) = \boldsymbol{\psi} e^{\lambda t} \tag{24}$$

The eigenvalue problem associated with the equations above is now in term of an asymmetric matrix and can be expressed as

$$\underset{\sim}{\mathbf{A}}_c \boldsymbol{\psi} = \lambda \boldsymbol{\psi} \tag{25}$$

where $\boldsymbol{\psi}$ is a complex eigenvector and its dimension is 2*N*, and λ is a complex parameter.

Considering an under-damped system, that is the case in most civil structures, the 2*N* eigenvalues are obtained in couples like these:

$$\lambda_{2j-1}, \lambda_{2j} = -\omega_j \zeta_j \pm i\omega_j \sqrt{1-\zeta_j^{\,2}}\ , \tag{26}$$

where *j* is the index of the mode, ω_j and ζ_j are the frequency of the undamped system corresponding to the j-th mode.

2.2.4 Output vectors

We are going to introduce the output vectors representation because the System Identification in order to obtain the modal parameters of the structures refers to measurements (output vectors) from dynamic tests done in field just at some specific points.

Supposing that the number of sensors be equal to *l*, including velocity, acceleration and displacement transducers. Hence we can write the output vector $\mathbf{y}(t)$ associated with the equation of motion:

$$\mathbf{y}(t) = \underset{\sim}{\mathbf{C}}_a \ddot{\mathbf{v}}(t) + \underset{\sim}{\mathbf{C}}_v \dot{\mathbf{v}}(t) + \underset{\sim}{\mathbf{C}}_d \mathbf{v}(t) \tag{27}$$

where the $\underset{\sim}{\mathbf{C}}_a, \underset{\sim}{\mathbf{C}}_v$ e $\underset{\sim}{\mathbf{C}}_d$ are matrices used to identify the degrees of freedom involved in the tests. The elements of the matrices above are all equal to zero despite of the ones corresponding to the *i*-th degree of freedom where the instrument gets the measurement.

Using the equations of motion and the output vectors, we can represent the mechanic system in the second order form:

$$\underset{\sim}{\mathbf{M}}\ddot{\mathbf{v}}(t) + \underset{\sim}{\mathbf{C}}\dot{\mathbf{v}}(t) + \underset{\sim}{\mathbf{K}}\mathbf{v}(t) = \mathbf{f}(t) \tag{28}$$

$$\mathbf{y}(t) = \underset{\sim}{\mathbf{C}}_a \ddot{\mathbf{v}}(t) + \underset{\sim}{\mathbf{C}}_v \dot{\mathbf{v}}(t) + \underset{\sim}{\mathbf{C}}_d \mathbf{v}(t) \tag{29}$$

Introducing the following statements:

$$\underset{\sim}{\mathbf{C}} = \left[\underset{\sim}{\mathbf{C}}_d - \underset{\sim}{\mathbf{C}}_a \underset{\sim}{\mathbf{M}}^{-1} \underset{\sim}{\mathbf{K}} \quad \underset{\sim}{\mathbf{C}}_v - \underset{\sim}{\mathbf{C}}_a \underset{\sim}{\mathbf{M}}^{-1} \underset{\sim}{\mathbf{C}} \right] \tag{30}$$

$$\mathbf{D} = \mathbf{C}_a \mathbf{M}^{-1} \tag{31}$$

the equations (24) and (25) can be written in a form that is suitable for the first-order system as:

$$\mathbf{y}(t) = \underset{\sim}{\mathbf{C}}\mathbf{x}(t) + \underset{\sim}{\mathbf{D}}\mathbf{u}(t) \tag{32}$$

The $\underset{\sim}{\mathbf{C}}$ e $\underset{\sim}{\mathbf{D}}$ matrices select the observed signal from the corresponding internal states and they are equivalent to coefficients matrices. They have a dimension of $l \times 2N$ and $l \times N$, respectively. It is possible now to introduce the state form for the representation of the mechanical system above:

$$\begin{aligned} \dot{\mathbf{x}}(t) &= \underset{\sim}{\mathbf{A}}_c \mathbf{x}(t) + \underset{\sim}{\mathbf{B}}_c \mathbf{u}(t) \\ \mathbf{y}(t) &= \underset{\sim}{\mathbf{C}}\mathbf{x}(t) + \underset{\sim}{\mathbf{D}}\mathbf{u}(t) \end{aligned} \tag{33}$$

2.2.5 System model in a discrete state-space form

The equations (29) are the continuous time equation of motion in the state space form for a linear time invariant N-DOF model under a generic force $\mathbf{u}(t)$.

The measurements, in term of displacement, velocity and acceleration, are obtained at a specific time interval and therefore, are in a discrete form. We have to treat the complex structural system as a discrete dynamic system subjected to excitation at a discrete locations and time steps. The model's identification problem consist on the determination of an $2N$ order system with the system matrices $\underset{\sim}{\mathbf{A}}_c$ and $\underset{\sim}{\mathbf{B}}_c$, using the

out-put measurements y(0), y(1), y(2),…..,y(s-1) obtained for s time steps [Peeters 1999].

Supposing that the solution at the generic step t_0 is known, we can find the solution at the following step t by the Lagrange formula.

$$\mathbf{x}(t) = \mathbf{x}_L(t) + \mathbf{x}_F(t) \tag{34}$$

where

$$\mathbf{x}_L(t) = e^{\mathbf{A}_c(t-t_0)}\mathbf{x}(t_0) \tag{35}$$

is the component of $\mathbf{x}(t)$ given by the free vibration solution of the system and

$$\mathbf{x}_F(t) = \int_{t_0}^{t} e^{\mathbf{A}_c(t-\tau)}\mathbf{B}_c\mathbf{u}(t)\,\mathrm{d}\tau \tag{36}$$

is the contribution to x(t) induced by the forcing function $\mathbf{u}(t)$. Using the equations above and assuming

$$t_0 = k\Delta t \;\; ; \quad t = (k+1)\Delta t \tag{37}$$

where k is an integer and represents the sampling instant and Δt is the sampling time, we can derive the discrete time of the state space equations in the form:

$$\begin{aligned} \mathbf{x}_{k+1} &= \underset{\sim}{\mathbf{A}}\mathbf{x}_k + \underset{\sim}{\mathbf{B}}\mathbf{u}_k \\ \mathbf{y}_k &= \underset{\sim}{\mathbf{C}}\mathbf{x}_k + \underset{\sim}{\mathbf{D}}\mathbf{u}_k \end{aligned} \tag{38}$$

The matrices $\underset{\sim}{\mathbf{A}}$ and $\underset{\sim}{\mathbf{B}}$ are defined as follow:

$$\underset{\sim}{\mathbf{A}} = e^{\underset{\sim}{\mathbf{A}}_c \Delta t} \tag{39}$$

$$\underset{\sim}{\mathbf{B}} = \int_0^{\Delta t} e^{\underset{\sim}{\mathbf{A}}_c \tau} \underset{\sim}{\mathbf{B}}_c \mathrm{d}\tau \quad = \underset{\sim}{\mathbf{A}}_c^{-1} [\underset{\sim}{\mathbf{A}} - \underset{\sim}{\mathbf{I}}] \underset{\sim}{\mathbf{B}}_c \tag{40}$$

The natural frequencies and the modal damping ratios can then be retrieved from the eigenvalues of $\underset{\sim}{\mathbf{A}}_c$ by the dynamic matrix in the discrete form $\underset{\sim}{\mathbf{A}}$, and the mode shapes can be evaluated using the corresponding eigenvectors and the output matrix $\underset{\sim}{\mathbf{C}}$ [Juang 1994]. Indicating with $\bar{\lambda}_j$ the generic eigenvalue of the $\underset{\sim}{\mathbf{A}}$ matrix, the natural frequency and the damping ratio are given by:

$$f_j = \frac{\left|\ln\left(\bar{\lambda}_j\right)\right|}{2\pi\Delta t} \tag{41}$$

$$\zeta_j = -\frac{\mathrm{Re}\left(\ln\left(\bar{\lambda}_j\right)\right)}{\left|\ln\left(\bar{\lambda}_j\right)\right|} \tag{42}$$

where j is the index of the mode, f_j is the frequency and ζ_j is the damping ratio corresponding to the jth mode. The jth complex mode shape ϕ_j sampled at sensor locations can also be evacuated using the following expression:

$$\phi_j = \underset{\sim}{\mathbf{C}} \psi_j \tag{43}$$

where ψ_j is the eigenvector of $\underset{\sim}{\mathbf{A}}$ corresponding to the eigenvalue $\bar{\lambda}_j$.

2.3 Signal analysis

This work focuses on output identification methods using the measurements from the tests on the footbridge for ambient and artificial loads. These data represent a random physical phenomenon and therefore they cannot be described by an explicit mathematical relationship, because each observation of the phenomenon will be unique. In other words, any given observation will represent only one of the possible outcome that might have occurred. We cannot know the exactly value that a random data will have in the future. The science which studies this type of data is called Statistics and it uses average quantities. We are going to define this kind of data and to introduce the instruments and the relations that join them in the following section. After that, the theory of Signal Analysis will be shown that is useful to define the frequency response function (FRF). Knowing these relations the dynamic and modal proprieties of the structure can be obtained.

2.3.1 Random data

A single time history representing a random phenomena is called sample; the collection of all possible sample functions is named random process or stochastic process. This kind of processes could be divided in the following categories:

1. stationary processes: they are random processes where all of their statistical properties do not change with time. They may be further categorized as being ergodic or not ergodic. For ergodic random process the time-averaged mean value and autocorrelation function, that we will show later, are equal to the corresponding ensemble averaged values.

2. non-stationary random processes: the properties of non stationary random process are generally time-varying functions that can be determined only by performing instantaneous averages over the ensemble of sample functions forming the process.

The properties of the random data are described by four types of statistical functions: the averaged square value, the spectral density function, the auto-correlation function and the density spectrum power function. In order to describe these proprieties the basic tools and equations which define the random data will be introduced:

The **Mean Value** μ_x of the time history of a random process *x(t),* is defined as follow:

$$\mu_x = \lim_{T\to\infty} \frac{1}{T} \int_0^T x(t)\mathrm{dt} \tag{44}$$

where *T* is the sample period.

The **Mean Square Value** Ψ_x^2 of the time history of a casual process *x(t),* is described by the following expression at it represent an approximation of the intensity of the time history:

$$\Psi_x^2 = \lim_{T\to\infty} \frac{1}{T} \int_0^T x^2(t)dt \tag{45}$$

It is useful to consider the data as a composition of a static component, not variable with time, that is the men value, and of a dynamic component, introducing the variance.

$$\sigma_x^2 = \Psi_x^2 - \mu_x^2 \tag{46}$$

The **Variance** could be written also in the following way:

$$\sigma_x^2 = \lim_{T\to\infty} \frac{1}{T} \int_0^T \left[x(t) - \mu_x\right]^2 dt \tag{47}$$

The variance of a random variable, or a probability distribution is a measure of statistical dispersion from the expected value.

The **probability density function.** This function represents the probability that *x(t)* assumes a specific value in a known interval x and $x+\Delta x$; this function could be valuated also by the ratio between T_x and T where the first one is the total time in which *x(t)* is in the interval ($x,\ x+\Delta x$) and T is the period of observation.

$$p(x)=\lim_{\Delta x\to\infty}\frac{\Pr ob\left[x\langle x(t)\langle x+\Delta x\right]}{\Delta x}=\lim_{\Delta x\to\infty}\frac{1}{\Delta x}\left[\lim_{T\to\infty}\frac{T_x}{T}\right] \tag{48}$$

Now it is possible to write the mean and the mean square values by the following expressions respectively (equations 45 and 46).

$$\mu_x=\int_{-\infty}^{\infty}x\cdot p(x)dx \tag{49}$$

$$\Psi_x^2=\int_{-\infty}^{\infty}x^2\cdot p(x)dx \tag{50}$$

In order to introduce the other random data features, we will show before the tools and equations of the signal analysis.

2.3.2 The Fourier series and transforms

The Fourier Transform (FT) defines a relationship between a signal in the time domain and its representation in the frequency domain. Being a transform, no information is created or lost in this process, so the original signal can be recovered from knowing the Fourier transform, and vice versa.

If the signal is periodic, in other words if $x(t) = x(t+T_0)$ for every instant t, considering T_0 the signal period, it can be written as a sum of harmonic functions using the Fourier transform:

$$x(t) = \sum_{k=-\infty}^{\infty} X_k(\omega) e^{jk\omega t} \tag{51}$$

where the X_k coefficients are given by the following expression:

$$X_k(\omega) = \frac{1}{T_0} \int_{-\frac{T_0}{2}}^{\frac{T_0}{2}} x(t) \cdot e^{-jk\frac{2\pi}{T_0}t} \, \mathrm{d}t$$

and $j = \sqrt{-1}$

(52)

If the function $x(t)$ could not be considered periodic, we will have a more generic expression of the Fourier transform and it is represented as follow:

$$X_k(\omega) = \int_{-\infty}^{\infty} x(t) \cdot e^{-j\omega t} \, \mathrm{d}t \tag{53}$$

In order to get the Fourier coefficient corresponding to the *k-th* harmonic function, using discrete time steps Δt, it is necessary to round up/down the expression above in the following way:

$$X_k = \frac{1}{N\Delta t} \sum_{n=0}^{N-1} x(n\Delta t) \cdot e^{-jk\frac{2\pi}{N\Delta t}n\Delta t} = \frac{1}{N\Delta t} C_k, \tag{54}$$

where

$$C_k = \sum_{n=0}^{N-1} x(n\Delta t) \cdot e^{-\frac{j\,2\pi\;k\;n}{N}}$$

(55)

is the Discrete Fourier transform (DFT) or Fast Fourier Transform (FFT) and N is the number of the time steps.

The DFT creates spectra where each value could be considered as the output of a filter centred at the ω frequency. The FT when n=0

$$X_0 = \frac{1}{N} \sum_{n=0}^{N-1} x(n\Delta t)$$

(56)

is the mean value of the x signal.

2.3.3 Autocorrelation function

In Statistics, the autocorrelation of a random process describes the correlation between values of the process at different points in time, as a function of the two times or of the time difference.

Given a time history *x(t),* the autocorrelation function of it is the continuous cross-correlation integral of *x(t)* with itself a time t and $t+\tau$ and it could be written:

$$R_{xx}(\tau) = \lim_{T\to\infty} \frac{1}{T} \int_0^T x(t)x(t+\tau)dt$$

(57)

If the function R is well-defined, its value must lie in the range [−1, 1], with 1 indicating perfect correlation and −1 indicating perfect anti-correlation.

The discrete autocorrelation R_{xx} at lag j for a discrete signal x_n is

$$R_{xx}(j) = \sum_{n} x_n x_{n-j} \tag{58}$$

It is real, symmetric and positive and it has a maximum at $\tau = 0$.

It is also correlated with the mean square value and the average value as:

$$\mu_x = \sqrt{R_{xx}(0)}$$
$$\Psi_x^2 = R_{xx}(0) \tag{59}$$

Thus, the autocorrelation function of a waveform is a similarity between the waveform and a time-shifted version of itself, as a function of this time shift.

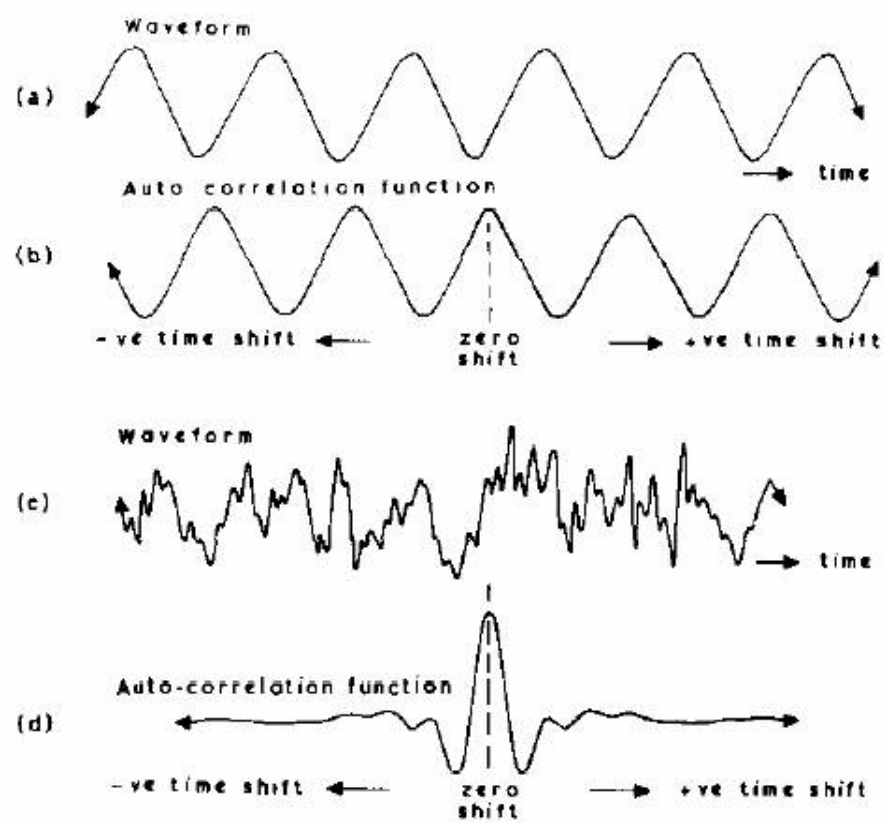

Figure1.18. Autocorrelation of two different waveforms

The autocorrelation of a periodic function is periodic, the autocorrelation of a random signal instead tends to zero for $\tau \neq 0$.

2.3.4 The Power Spectral Density function (PSD)

The Fourier transformation of the autocorrelation function $R_{xx}(\tau)$ is called Power Spectral density function (PSD), or auto-spectrum:

$$S_{xx}(\omega) = \int_{-\infty}^{+\infty} R_{xx}(\tau) e^{-j\omega\tau} d\tau \tag{60}$$

The function $\boldsymbol{S}_{xx}(\omega)$ is obtained by the Fourier transformation $X(\omega)$ of the time history $x(t)$ using the following relation:

$$S_{xx}(\omega) = \bar{X}(\omega) X(\omega) \tag{61}$$

Where $\bar{X}(\omega)$ is the complex conjugate of $X(\omega)$. $S_{xx}(\omega)$ is a real function and contains the frequencies' information of $x(t)$, but doesn't give information about the phases because it is obtained just from the module of $X(\omega)$.

2.3.5 The cross correlation function

The cross correlation function describes the correlation between two set of data. Indicating with *x(t)* the first set and with *y(t)* the second set of random data, the cross correlation function is the product of *x(t)* at the time *t* with *y(t)* at time $t+\tau$ for an appropriate averaging time *T* and is given by the following expression:

$$R_{xy}(\tau) = \lim_{T\to\infty} \frac{1}{T} \int_0^T x(t) y(t+\tau) dt \tag{62}$$

where τ is a constant time delay.

The R_{xy} function is always real, positive or negative but it doesn't have a maximum at $\tau = 0$.

2.3.6 Cross-spectral density function

The Fourier Transformation of the cross-correlation function R_{xy} is called cross-spectrum (CSD) and it is usually indicated by $S_{xy}(\omega)$:

$$S_{xy}(\omega) = \int_{-\infty}^{+\infty} R_{xy}(\tau) e^{-j\omega\tau} d\tau \tag{63}$$

The $S_{xy}(\omega)$ function is obtained by the Fourier transformation of both $x(t)$ and $y(t)$ using the following expression:

$$S_{xy}(\omega) = \overline{X}(\omega) Y(\omega) \tag{64}$$

This is a complex function and both the information about frequencies and phases are contained. Its amplitude is the product of the two amplitudes, and the phase the difference of the two phases (from $X(\omega)$ to $Y(\omega)$). The real part is known as the "coincident or co-spectrum" and it gives a measure of how well the two functions correlate as a function of frequency, while the imaginary part is termed the "quadrature or quad-spectrum" and angle a measure of the phase shift between the two signals as a function of frequency.

2.3.7 Coherence

The coherence gives a measure of the degree of linear dependence between the two signals, as a function of frequency. It compares the out-put with the in-put and produces the coherence factor.

$$\gamma^2(\omega) = \frac{\left|S_{yx}(\omega)\right|^2}{S_{yy}(\omega)\,S_{xx}(\omega)}.$$

(65)

If $\gamma^2(\omega) < 0.75$ the experimental measures aren't really good because the ratio signal/ noise is low. There are also other things like the non linear behaviour of the structure or some missing measurements that could produce a low value of ratio and coherence.

2.3.8 The frequency response functions (FRF)

It is really important to introduce the frequency response functions (FRF). For a constant-parameter linear system, the FRF $H(\omega)$ is the Fourier transform of a *unit impulse response function h(t)* :

$$H(\omega) = \int_0^\infty h(t) \cdot e^{-j2\pi f\tau} d\tau$$

(66)

where $h(t) = 0 \quad for \quad \tau < 0$

(67)

The signal could be considered like a sum of unit impulse. Therefore, considering the force $f(t)$ pressing the structure and $y(t)$ the response, we can obtain the FRF for every couple consisting of excitation and response by the ratio of Fourier Transform of the response $Y(\omega)$ and of the force $F(\omega)$:

$$H(\omega) = \frac{Y(\omega)}{F(\omega)}.$$

This is sometime known as "transfert function".

(68)

2.3.9 Frequency response functions in term of displacement, velocity and acceleration

The FRF are generally represented like the ratio between the Fourier transform of the out-put (in term of displacement, velocity, force, acceleration) and the Fourier transform of the force module. First of all we can define the *receptance* function α that is the ratio between the displacement transform *y(t)* of a generic point of the system and the Fourier transform of the applied force *f(t)*:

$$\alpha(\omega) = \frac{Y(\omega)}{F(\omega)}.$$

(69)

At the same way we can introduce the *mobility* function that consist of the ratio between the velocity out-put $\dot{y}$ of a generic point of the system and the Fourier transform of the force *f*(*t*).

$$B(\omega) = \frac{\dot{Y}(\omega)}{F(\omega)}$$

(70)

To conclude, we give also the expression of the *inertance* that is the ratio between the acceleration out-put $\ddot{y}$ of a generic point of the system and the FT of the force *f*(*t*).

$$A(\omega) = \frac{\ddot{Y}(\omega)}{F(\omega)}.$$

(71)

These first and the third expressions could be join in the following way.

$$A(\omega) = -\omega^2 \cdot \alpha(\omega)$$

(72)

We use the last two formulas because the output data are in term of accelerations.

2.3.10 The frequency response function for N-DOF systems

For *N*-degree of freedom systems with viscous damping, the equations of motion assume the following form:

$$\underset{\sim}{\mathbf{M}}\ddot{\mathbf{v}} + \underset{\sim}{\mathbf{C}}\dot{\mathbf{v}} + \underset{\sim}{\mathbf{K}}\mathbf{v} = \mathbf{f} .$$

(73)

Calculating the Fourier transform of both the parts, we obtain the following result:

$$\int_{-\infty}^{\infty} \left(\underset{\sim}{\mathbf{M}}\ddot{\mathbf{v}} + \underset{\sim}{\mathbf{C}}\dot{\mathbf{v}} + \underset{\sim}{\mathbf{K}}\mathbf{v}\right) \cdot \boldsymbol{e}^{-i\omega t} \mathrm{d}\boldsymbol{t} = \int_{-\infty}^{\infty} \mathbf{f} \cdot \boldsymbol{e}^{-i\omega t} \mathrm{d}\boldsymbol{t}$$

(74)

That could be written also as:

$$\left(-\omega^2 \cdot \underset{\sim}{\mathbf{M}} + \boldsymbol{i}\omega \cdot \underset{\sim}{\mathbf{C}} + \underset{\sim}{\mathbf{K}}\right) \cdot \mathbf{V}(\omega) = \mathbf{F}(\omega)$$

(75)

where $\mathbf{V}(\omega)$ and $\mathbf{F}(\omega)$ are the Fourier transforms of the displacement **v** and the force **f**.

The receptance could be written as follow:

$$\underset{\sim}{\boldsymbol{\alpha}}(\omega) = \left(-\omega^2 \cdot \underset{\sim}{\mathbf{M}} + i\omega \cdot \underset{\sim}{\mathbf{C}} + \underset{\sim}{\mathbf{K}}\right)^{-1}. \tag{76}$$

Recalling the modal matrix $\underset{\sim}{\boldsymbol{\varphi}}$ that has in columns the eigenvectors and using the well known expressions of orthogonal modes of vibration systems

$$\underset{\sim}{\boldsymbol{\varphi}}^t \ \underset{\sim}{\mathbf{K}} \ \underset{\sim}{\boldsymbol{\varphi}} = \boldsymbol{diag}(\omega_r^2), \tag{77}$$

$$\underset{\sim}{\boldsymbol{\varphi}}^t \ \underset{\sim}{\mathbf{M}} \ \underset{\sim}{\boldsymbol{\varphi}} = \underset{\sim}{\mathbf{I}}, \tag{78}$$

$$\underset{\sim}{\boldsymbol{\varphi}}^t \ \underset{\sim}{\mathbf{C}} \ \underset{\sim}{\boldsymbol{\varphi}} = \boldsymbol{diag}(2\zeta_r\omega_r), \tag{79}$$

it is possible to write the equation of motion in this other way:

$$\underset{\sim}{\boldsymbol{\varphi}}^t \ \underset{\sim}{\boldsymbol{\alpha}}(\omega)^{-1} \ \underset{\sim}{\boldsymbol{\varphi}} = \underset{\sim}{\boldsymbol{\varphi}}^t \left(-\omega^2 \cdot \underset{\sim}{\mathbf{M}} + i\omega \cdot \underset{\sim}{\mathbf{C}} + \underset{\sim}{\mathbf{K}}\right) \underset{\sim}{\boldsymbol{\varphi}}, \tag{80}$$

$$= diag\left(\omega_r^2 - \omega^2 + 2i\zeta_r\omega_r\omega\right),$$

Finally receptance could be written:

$$\underset{\sim}{\boldsymbol{\alpha}}(\omega) = \underset{\sim}{\boldsymbol{\varphi}}^t \boldsymbol{diag}\left(\omega_r^2 - \omega^2 + 2 \ \boldsymbol{i} \ \zeta_r\omega_r\omega\right)^{-1} \ \underset{\sim}{\boldsymbol{\varphi}}. \tag{81}$$

or in components:

$$\alpha_{jk}(\omega) = \sum_{r=1}^{N} \frac{\phi_{rj}\,\phi_{rk}}{\left(\omega_r^2 - \omega^2 + 2i\zeta_r\omega_r\omega\right)}. \tag{82}$$

The inertance function for this case derivers from the expression (76):

$$A_{jk}(\omega) = -\sum_{r=1}^{N} \frac{\omega^2 \cdot \phi_{rj}\,\phi_{rk}}{\left(\omega_r^2 - \omega^2 + 2i\,\zeta_r \omega_r \omega\right)}\,, \tag{83}$$

The formula above (1.66) could be written also as follow:

$$A_{jk}(\omega) = -\sum_{r=1}^{N} \frac{\omega^2 \cdot \left(R_{jk}\right)_r}{\left(\omega_r^2 - \omega^2 + 2i\,\zeta_r \omega_r \omega\right)} \tag{84}$$

Where R_{jk} is the residue and it is given by the product of the eigenvectors.

2.3.11 FRF in the state form

It is our aim now to write the same expression in an other form. Starting from the well known equation of motion in the sate form will have :

$$\dot{\underset{\sim}{\mathbf{x}}}(t) = \underset{\sim}{\mathbf{A}}_c \mathbf{x}(t) + \underset{\sim}{\mathbf{B}}_c \mathbf{u}(t) \tag{85}$$

and assuming an harmonic excitation and the corresponding harmonic response of the structure we reach the following expression:

$$\left(i\omega \underset{\sim}{\mathbf{I}} - \underset{\sim}{\mathbf{A}}_c\right)\mathbf{X}e^{i\omega} = \underset{\sim}{\mathbf{B}}_c \mathbf{U}e^{i\omega} \tag{86}$$

from this is easy to obtain the FRF of the displacement:

$$\underset{\sim}{\boldsymbol{\alpha}}(\omega) = \left(\boldsymbol{i}\omega\underset{\sim}{\mathbf{I}} - \underset{\sim}{\mathbf{A}}_c\right)^{-1}$$

(87)

Using the pre-multiplication and the post-multiplication of the two sides with the eigenvector $\boldsymbol{\psi}$ we obtain:

$$\underset{\sim}{\boldsymbol{\psi}}\ \ \underset{\sim}{\boldsymbol{\alpha}}(\omega)^{-1}\underset{\sim}{\boldsymbol{\psi}} = \underset{\sim}{\boldsymbol{\psi}}\left(\boldsymbol{i}\omega\underset{\sim}{\mathbf{I}} - \underset{\sim}{\mathbf{A}}_c\right)\underset{\sim}{\boldsymbol{\psi}}$$

(88)

Are now introduced the proprieties of orthogonal modes of vibration systems and the above formula is written by its components:

$$\alpha_{jk}(\omega) = \sum_{r=1}^{2N}\frac{\psi_{jr}\psi_{kr}}{(i\omega - \lambda_r)}$$

(89)

The sum of the equation above extends $2N$ because the equation $\dot{\mathbf{x}}(t) = \mathbf{A}_c\mathbf{x}(t) + \mathbf{B}_c\mathbf{u}(t)$ consist of $2N$ components. The eigenvectors are N conjugate couples and therefore the expression above could be also written as follow:

$$\alpha_{jk}(\omega) = \sum_{r=1}^{N}\left[\frac{\psi_{jr}\psi_{kr}}{(i\omega - \lambda_r)} - \frac{\psi_{jr}^{*}\psi_{kr}^{*}}{(i\omega - \lambda_r^{*})}\right],$$

(90)

where the complex conjugate member is indicated with the(*) symbol.

The FRF have a relevant importance in the System identification.

2.4 Instrumentation for the frequency domain

Appropriate techniques for the acquisition and processing of random data are heavily dependent on the physical phenomenon represented by the data and the desired engineering goals of the processing. In broad terms, however, the required operations may be divided into five primary categories: data collection, data recording (including transmission), data preparation, data qualification and data analysis. Each of these categories involves a number of sequential steps. During these steps we some sources of errors can occur.

2.4.1 Aliasing

In the digitalization of a continuous signal, the sampling of the signal is obtained for equal time steps. The problem is to find a good sampling interval. On the one hand, sampling with steps that are too close each other will lead to have too many data and to an increasing in the computational calculus. On the other hand, if the sampling frequency is too low we couldn't get the real wave of the signal.

Aliasing is a phenomenon in analog to digital conversion in which the frequency of the converted signal is lower than that of the original signal. This latter problem constitutes a potential source of error that does not arise in direct analog data processing, but is inherent in all digital processing that is preceded by an analog to digital conversion. It is often overlooked, sometimes with disastrous results.

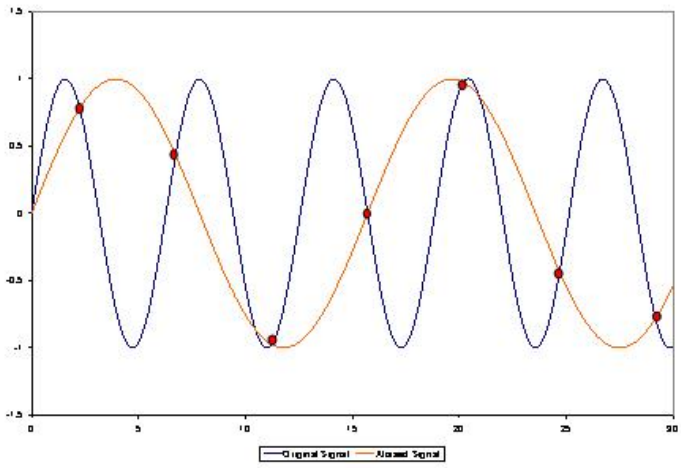

Figure1.19. example of Aliasing, the signal is not correcting digitalized

This minimum sample rate requirement is known as the Nyquist Criterion. In the time domain a sampling frequency exactly twice the input frequency would not always be enough. Whereas, slightly more than two samples in each period gives sufficient information. It certainly would not be enough to give a high quality time display. The Nyquist Criterion of a sample rate greater than twice the maximum input frequency is sufficient to avoid aliasing and preserve all the information in the input signal.

Therefore the higher frequency that could be define by the sampling ration of $1/\Delta t$ samples over second is

$$f_c = \frac{1}{2\Delta t}. \qquad (91)$$

This cutting or band-limiting frequency is called ***Nyquist frequency***.

The aliasing problem could be solved using a filter (or our FFT processor which acts like a filter) after the sampler. It will remove the alias products while passing the desired input signals if the sample rate is greater than twice the highest frequency of the input. If the sample rate is lower, the alias products will fall in the frequency range of the input and no amount of filtering will be able to remove them from the signal.

2.4.2 Leakage

Leakage describes an unwanted loss, or leak, of something which escapes from its proper location.

In everyday usage, *leakage* is the gradual escape of matter through a leak-hole.

In our case, we have seen that the spectrum of a frequency response depend also of the time of observation T therefore the leakage is a problem connected with the length of the time history and the assumption of a periodic signal.

If the time record contains an integral number of cycles of the input sine wave, then this assumption exactly matches the actual input waveform as shown in Figure 2.4. In this case, the input waveform is said to be periodic in the time record.

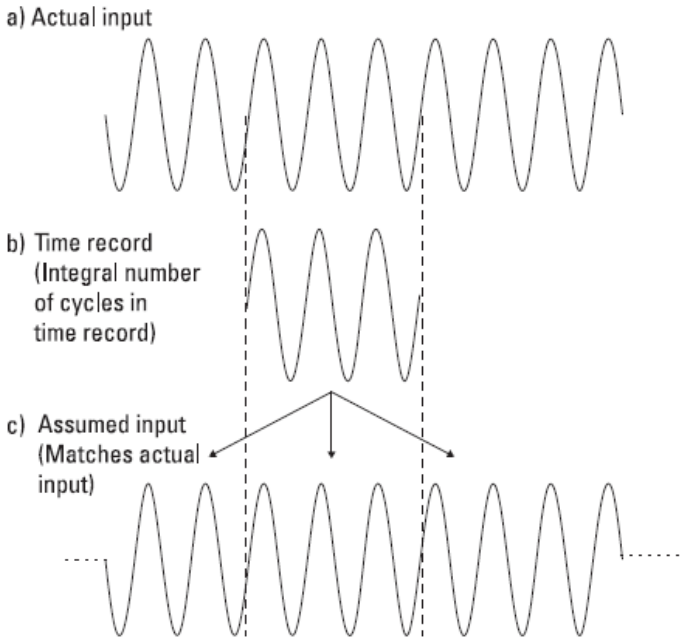

Figure1.20. Input signal periodic in time record

Figure 2.5 demonstrates the difficulty with this assumption when the input is not periodic in the time record. The FFT algorithm is computed on the basis of the highly distorted waveform in Figure 2.5c. The actual sine wave input has a frequency spectrum of single line. The spectrum of the input assumed by the FFT in Figure 2.5c should be very different. Since sharp phenomena in one domain are spread out in the

other domain, we would expect the spectrum of our sine wave to be spread out through the frequency domain.

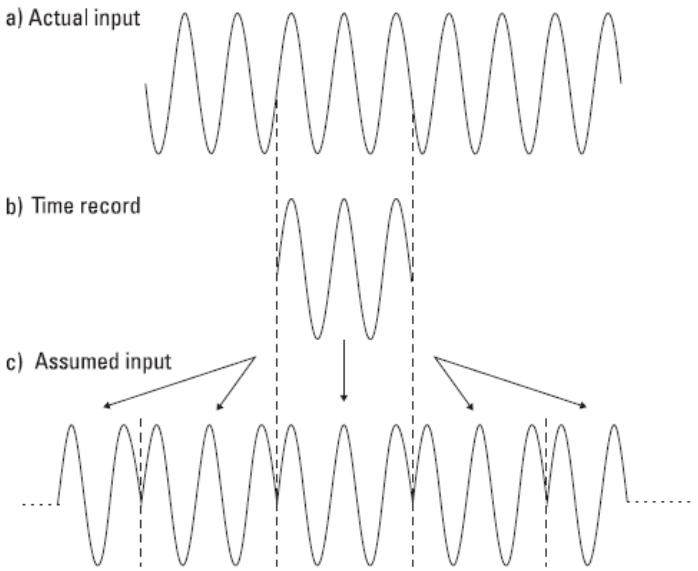

Figure1.21. Input signal not periodic in time record

In Figure 2.6 we see in an actual measurement that our expectations are correct. In Figures 2.6 a & b, we see a sine wave that is periodic in the time record. Its frequency spectrum is a single line whose width is determined only by the resolution of our Dynamic Signal Analyzer. On the other hand, Figures 2.6 c & d show a sine wave that is not periodic in the time record. Its power has been spread throughout the spectrum as we predicted. This smearing of energy throughout the frequency domains is a phenomenon known as ***leakage***.

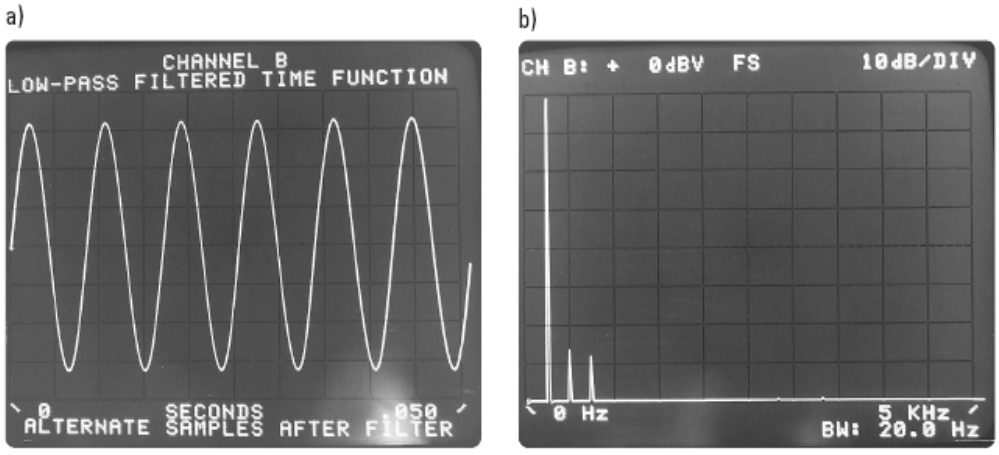

a) & b) Sine wave periodic in time record

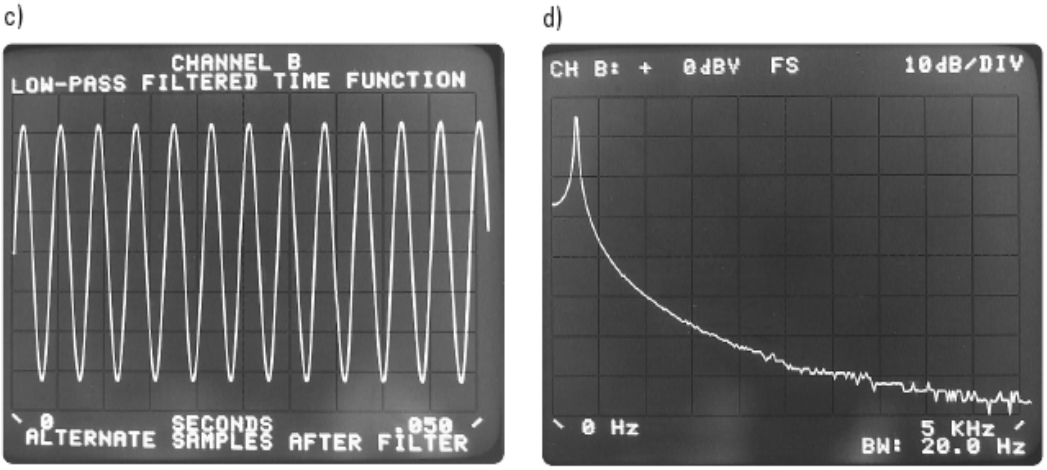

c) & d) Sine wave not periodic in time record

Figure1.22. Actual FFT results

We are seeing energy leak out of one resolution line of the FFT into all the other lines. It is important to realize that leakage is due to the fact that we have taken a finite time record. For a sine wave to have a single line spectrum, it must exist for all time, from minus infinity to plus infinity. If we were to have an infinite time record, the FFT would compute the correct single line spectrum exactly. However we need to look at a finite time record of the sine wave for evident reasons. This can cause leakage if the continuous input is not periodic in the time record. It is obvious from Figure 2.6 that the problem of leakage is severe enough to entirely mask small signals close to our sine waves. As such, the FFT would not be a very useful spectrum analyzer.

If there are two sinusoids, with different frequencies, leakage can interfere with the ability to distinguish them spectrally. If their frequencies are dissimilar, then the leakage interferes when one sinusoid is much smaller in amplitude than the other. That is, its spectral component can be hidden by the leakage from the larger component. But when the frequencies are near each other, the leakage can be sufficient to interfere even when the sinusoids are equal strength; that is, they become *irresolvable*.

2.4.3 Windowing

Windowing is a method used to solve the leakage problem. It is able to filter the in-put signal x(t) using a filtering function W(t). This operation, called windowing, gives a signal $x'(t) = W(t) \cdot x(t)$ that help to reduce the spectral dispersion.

In Figure 2.7 we have again reproduced the assumed input wave form of a sine wave that is not periodic in the time record. Notice that most of the problem seems to be at the edges of the time record, the centre is a good sine wave. If the FFT could be made to ignore the ends and concentrate on the middle of the time record, we would expect to get much closer to the correct single line spectrum in the frequency domain. If we multiply our time record by a function that is zero at the ends of the time record and large in the middle, we would concentrate the FFT on the middle of the time record. One such function is shown in Figure 2.7c. Such functions are called window functions because they force us to look at data through a narrow window.

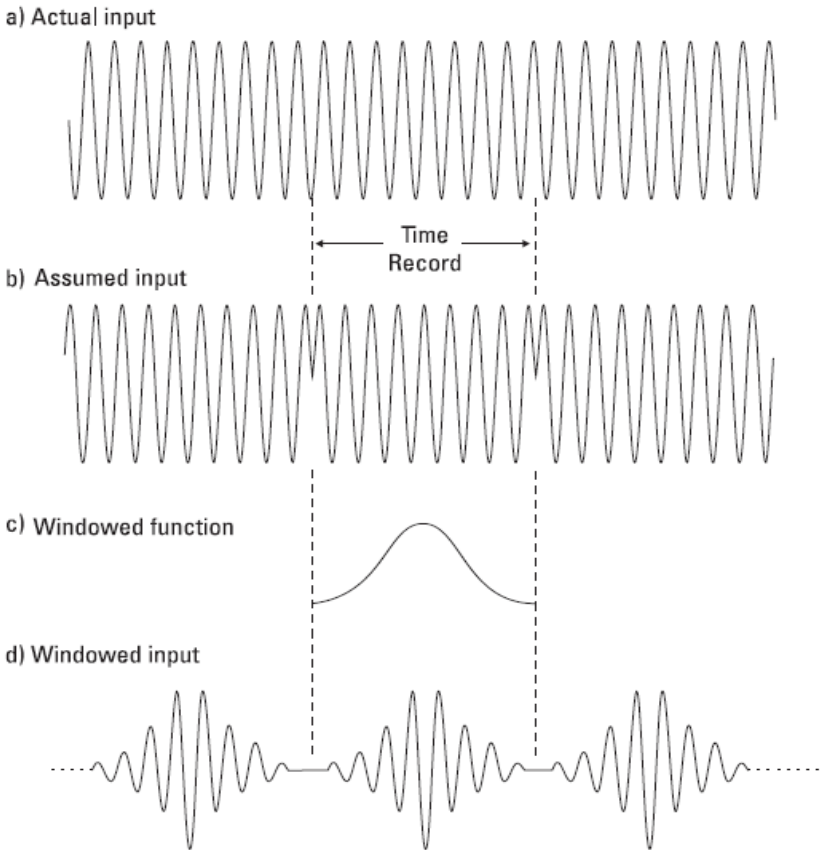

Figure1.23. The effect of windowing in the time domain

Figure 2.8 shows us the vast improvement we get by windowing data that is not periodic in the time record. However, it is important to realize that we have tampered with the input data and cannot expect perfect results. The FFT assumes the input looks like Figure 2.8c, something like an amplitude-modulated sine wave in the time record.

a) Sine wave not periodic in time record

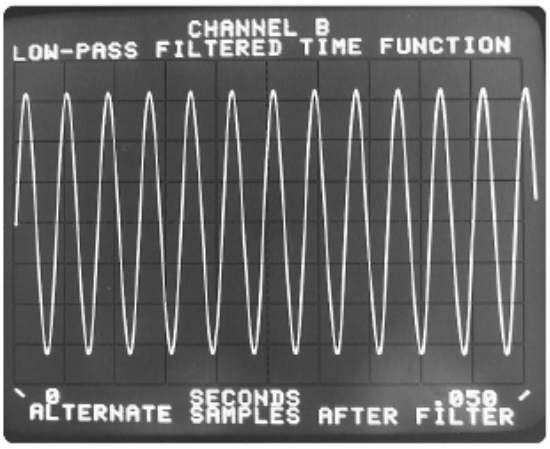

b) FFT results with no window function

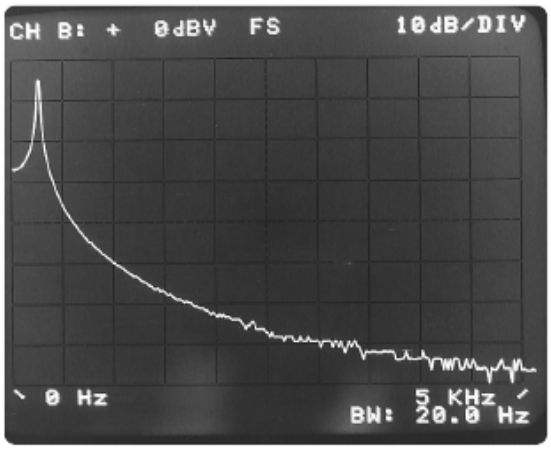

c) FFT results with a window function

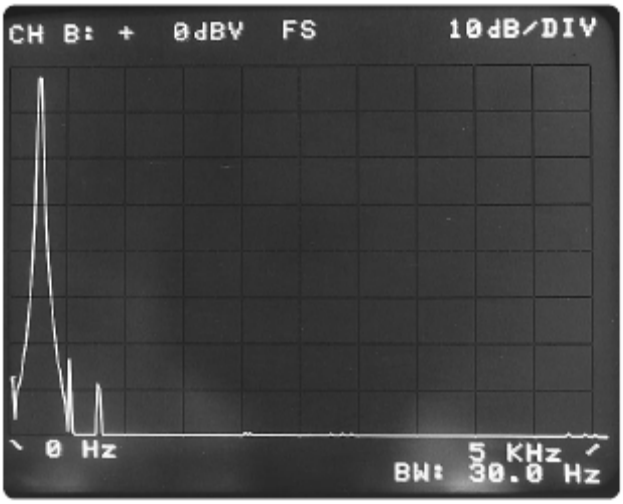

Figure1.24. Leakage reduction with windowing

This has a frequency spectrum which is closer to the correct single line of the input sine wave than Figure 2.6b, but it still is not correct. Figure 2.9 demonstrates that the windowed data does not have as narrow a spectrum as an unwindowed function which is periodic in the time record.

a) Leakage-free measurement - input periodic in time record

b) Windowed measurement - input not periodic in time record

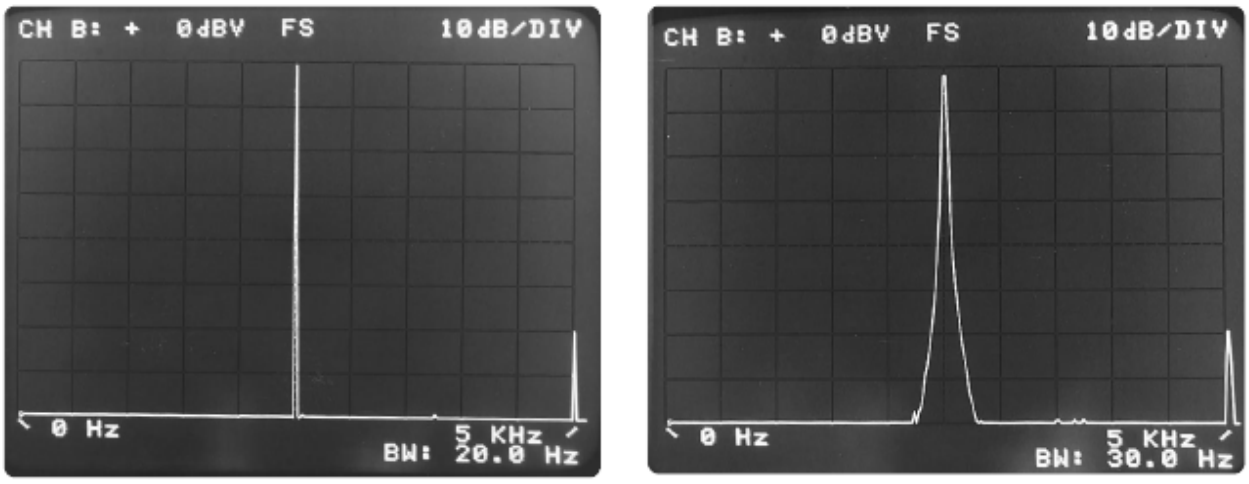

Figure1.25. Windowing reduces leakage but does not eliminate it

There are a lot of different windows and following there is a list of the most important ones:

- ✓ Box window
- ✓ Hamming Window;
- ✓ Cosine Taper Window;
- ✓ Exponential Window.

Every window corresponds to a specific type of signal, for example the second and the third are
used for periodic signals or for random vibrations; the fourth one is used for transient state in which
the more important data are concentrated in a specific part of the whole signal.

2.4.4 Overlap averaging

From the figure 2.9 it is seen that windowing the time history, the leakage error is suppressed, but it also increase the width of the main lobe of the spectral window; that is, it reduces the basic resolving power of the analysis. For Hanning, the increase in the half-power bandwidth of the main lobe is about 60%. This is generally an acceptable penalty to pay for the suppression of the leakage from frequencies outside the region of the main lobe. However, there may be cases where maintaining a minimum main-lobe bandwidth is critical to the analysis. This can be achieved by simply increasing the record length T for each FFT to provide the same bandwidth with windowing that would have occurred without windowing.

To counteract the increase in variability caused by time-history windowing for leakage suppression, overlapped processing techniques are sometimes used.

Specifically, instead of dividing a record $x(t)$ into n_d independent segments, $x_i(t)$, $(i-1)T \le t \le iT,\ i = 1,2,....,n_d$, the record is divided into overlapped segments $\boldsymbol{x_i(t)}$ covering the time intervals:

$$\left[q(i-1)\right]T \le t \le \left[q(i-1)+1\right]T, \quad i = 1,2,....,(n_d/q) \qquad q < 1$$

(92)

A common selection in overlapped processing is $q = 0.5$, which produces 50% overlapping. This will retrieve about 90% of the stability lost due to the windowing operation but also will double the required number of FFT operation.

Chapter 3

Introduction

Modal parameter identification is a procedure to identify dynamic properties of a vibrating structure starting from modal tests. Modal parameters can be estimate from a variety of different measurements in different data domains (time and/or frequency domain). It allows us to obtain the modal parameters of the structure such as mode shapes, damping ratios, natural frequencies by the not destructive tests on fields. These measurements can include free-decays, forced responses, frequencies response functions or impulse response functions. The measurements can be generated with no measured inputs, single measured input or multiple measured inputs.

Most current modal parameter estimation techniques are based on the frequency response function (FRF) or, equivalently, impulse response function (IRF) obtained from the measured data. FRFs are typically found by Fast Fourier Transform. Excitation of structure by dynamic forces is usually required in order to apply frequency domain methods. Forces may be imposed, for example, by means of a mechanical shaker. Acceleration records at different frequencies are used to calculate the corresponding FRFs. From these, frequencies domain methods as MDOF Circle Fit Method can be used to identify frequencies, deformations and damping ratios of various modes.

In the input-output system identification the modal parameters are obtained by a special model which defines the frequency response function that means a function that connects the in-put with the out-put. The system identification based just on the out-put data obtained by the test is called **out-put only**. When the system identification is based only on out-put data, two problems recur:

- ✓ The excitation in unknown;
- ✓ The out-put is often affected by noise.

The principal concept of the out-put only system identification is that the unknown external load is assumed as composed by a virtual load called white noise. It is

supposed that the white noise does not act in the structural system. Therefore is it possible to identify the structural modes and the virtual mode due to the white noise separately.

The concept of output-only modal testing is not new but the development of this technique has a brief history. For several years people working in modal analysis have been performing output only modal identification using the commonly accepted fact that if only one mode contributes to a certain band of the cross spectral matrix, then any row or column in that matrix can be used as a mode shape estimate. By picking a peak in one of the spectral density functions one can get the mode shape from one of the columns or rows in the cross spectral matrix. This classical approach, also known as Basic Frequency Domain (BFD) technique, is based on the simple signal processing technique using a discrete Fourier transform, and hinges on the fact that well separated modes can be estimated directly from the matrix of the cross spectra.

In the case of closely spaced modes, it can be difficult to detect the modes and, even in the case where close modes are detected, estimated frequencies and mode shapes become heavily biased. Furthermore, the estimated frequencies are limited by the frequency resolution of the estimated spectral density and, in all cases, damping estimation is uncertain or impossible.

The main advantage of the classical i.e. BFD approach is that the structural properties can be easily found just by examining the density functions. The disadvantages associated with this approach are removed by another method called Frequency Domain Decomposition technique (FDD) that was extensively investigated by Ren and Zong and Brincker et al. Brincker R, Zhang L, Andersen P (2000 and 2003) .

This method contains all the advantages of the classical technique and also provides clear indication of harmonic components in the response signal. It has been described that the spectral matrix can be decomposed with the Singular Value Decomposition (SVD) method into a set of auto spectral density functions, each corresponding to a Single Degree of Freedom (SDOF) system. The FDD technique can effectively handle close modes and noise, however it cannot provide damping information.

The Enhanced Frequency Domain Decomposition (EFDD) is basically an extension of the FDD technique capable of providing damping information. In EFDD, the identified frequency function around each resonant peak is transferred back to the time

domain using Inverse Discrete Fourier and damping can be obtained by the logarithmic decrement of the correspond SDOF normalized autocorrelation function. This is the approach we used for our case of study. The results are right if the structure has a low damping, the load is really a white noise and the mode shapes of the matched modes are orthogonal. Otherwise they are approximated but good anyway.

Time domain methods are more flexible since any kind of dynamic excitation can be used, such as noise excitations or forces induced by impact of weights on the structure. Among them, autoregressive models and subspace methods are the most effective methods. Possibility of extracting modal parameters from recorded time signals, without the need of direct measurement of excitation force, is their main advantage. It can be shown, in fact, that a stochastic state-space model may represent a vibrating structure excited by a stationary white noise.

The first time-domain technique that really became known for serious output-only identification was introduced by Ibrahim and Milkulcik and is known as the Ibrahim Time Domain (ITD) method. Shortly after that the Polyreference time-domain method were introduced by Vold et al. and Vold and Rocklin. The Eigen Realization Algorithm (ERA) was developed by Juan and Pappa and later employed in space application. The last two techniques, i.e. Polyreference and ERA, use multiple inputs but ITD can also be formulated as a multiple input method as described by Fukuzono. Recently, Zhang et al. gave a common formulation for all these techniques. What they have in common is that they assume that a free response function can be obtained. These time domain techniques are all based on a function represented by exponential decay.

Recently a lot of research effort was spent to a more modern time-domain techniques called Stochastic Subspace Identification (SSI). Three different implementations of Stochastic Subspace Identification technique are: Unweighted Principal Component (UPC), Principal Component (PC), and Canonical Variate Analysis (CVA). These methods are time domain methods that directly work with time domain data, without any conversion to spectral functions. Subspace methods identify state-space models from input and output data by applying robust numerical techniques such as *QR* factorization, *SVD* and *least squares*. They are based on projection of the row space of

future outputs into the row space of past outputs and they do not need any optimization procedure. The algorithm for this new stochastic subspace time domain technique was described by Van Overschee and De Moor. Also, more detailed information on stochastic subspace method can be found in Pandit SM (1991) and Peeters B, De Roeck G (2001).

The main purpose of this thesis is the characterization of dynamic behaviour of structure using frequency domain methods. The EFDD method will be shown. Identified parameters are modal frequencies, mode shapes and damping ratios.

EFDD method (Enhanced Frequency Domain Decomposition)

The technique presented in this paper is a frequency domain decomposition (FDD) technique. It removes all the disadvantages associated with the classical approach, but keeps the important features of user friendliness and even improves the physical understanding by dealing directly with the spectral density function. Furthermore, the technique gives a clear indication of harmonic components in the response signals.

Taking the singular value decomposition (SVD) of the spectral matrix, the spectral matrix is decomposed into a set of auto spectral density functions, each corresponding to a single degree of freedom (SDOF) system. This result is exact in the case where the loading is white noise, the structure is lightly damped and when the mode shapes of close modes are geometrically orthogonal.

If these assumptions are not satisfied the decomposition into SDOF systems is approximate, but still the results are significantly more accurate than the results of the classical approach.

2.4.5 Frequency domain analysis

It is considered a system with r input $x_i(t)\ \ i=1,2,....r$ and an out-put **y(t)**. It is assumed that **y(t)** is the sum of each $y_i(t)$ obtained by the transform functions $h_i(t)$ for each input $x_i(t)$.

$$\mathbf{y(t)} = \sum_{i=1}^{r} y_i(t)$$

(93)

$$\left.\begin{array}{l} x_1(t) \to h_1(t) \to y_1(t) \\ x_2(t) \to h_2(t) \to y_2(t) \\ \ldots \\ x_r(t) \to h_r(t) \to y_r(t) \end{array}\right\} \to y(t)$$

(94)

Applying the integral of convolution is obtained:

$$y_i(t) = \int_0^{\infty} h_i(\tau) \cdot x_i(t-\tau) d\tau \Rightarrow \mathbf{y(t)} = \sum_{i=1}^{r} \int_0^{\infty} h_i(\tau) \cdot x_i(t-\tau) d\tau$$

(95)

The autocorrelation function, as shown in chapter two, could be represent by the following form:

$$\underset{\sim}{\mathbf{R}}_{\mathbf{y}}(\boldsymbol{\tau}) = \sum_{i=1}^{r} \int \int_0^{\infty} h_i(\xi) \cdot h_i(\eta) \cdot R_i x_i(\xi - \eta + \tau) d\xi d\eta$$

(96)

Using the Fourier transform, the power spectral density function (SPD) is obtained:

$$\underset{\sim}{\mathbf{G}}_{\mathbf{y}}(\mathbf{f}) = 2 \int_{-\infty}^{+\infty} \underset{\sim}{\boldsymbol{R}}_{\boldsymbol{y}}(\boldsymbol{\tau}) e^{-j2\pi f\tau} d\tau =$$

$$= \sum_i \sum_j \int_0^{\infty} h_i(\xi) e^{j2\pi f\xi} d\xi \cdot \to \int_0^{\infty} h_j(\eta) e^{j2\pi f\eta} d\eta \cdot \int_0^{\infty} R_{ij}(t) e^{-j2\pi ft} dt =$$

$$= \sum_{i=1}^{r} \sum_{j=1}^{r} \bar{H}_i(f) \cdot H_j(f) \cdot G_{ij}(f)$$

(97)

where the symbol "—" means the complex conjugate. If it is preferable writing the formula like a matrix, it is necessary to introduce the r-dimensional input vector ***x*(t)**:

$$\boldsymbol{x(t)} = [x_1(t), x_2(t), ..., x_r(t)]$$

(98)

the r-dimensional vector of the frequency response function **H**(*f*):

$$\boldsymbol{H(f)} = [H_1(f), H_2(f), ..., H_r(f)]$$

(99)

the r-dimensional vector of the cross spectrum of in-put $\boldsymbol{x_i(t)}$:

$$\boldsymbol{G_{xy}}(f) = [G_{x_1 y}(f), G_{x_2 y}(f), ..., G_{x_r y}(f)]$$

(100)

and the *r* x *r* matrix for each in-put $x_i(t)$:

$$\boldsymbol{G_{xx}}(f) = \begin{bmatrix} G_{x_1x_2}(f) & G_{x_1x_2}(f) & ... & G_{x_1x_r}(f) \\ G_{x_2x_1}(f) & & ... & G_{x_2x_r}(f) \\ ... & ... & ... & \\ G_{x_rx_1}(f) & G_{x_rx_2}(f) & ... & G_{x_rx_r}(f) \end{bmatrix}$$

Therefore the power spectral density function becomes:

$$\boldsymbol{\tilde{G}_y(f)} = 2\int_{-\infty}^{+\infty} R(\tau)\cdot e^{-j2\pi f\tau} d\tau = \sum_{i=1}^{r}\sum_{j=1}^{r} \bar{\tilde{H}}_i(f)\cdot \tilde{H}_j(f)\cdot G_{ij}(f)$$

(101)

At this point the equation could be written in the matrix form:

$$\boldsymbol{\tilde{G}_{yy}(f) = \tilde{H}(f) \times \tilde{G}_{xx}(f) \times \bar{\tilde{H}}^T(f)}$$

(102)

where the symbol "T" stands for transposed.

If the measurements registered are *m*, the matrices above represent the following quantities:

$\boldsymbol{G_{xx}(f)}$ **:** spectral density matrix of the in-put, which has a dimension of **r x r**;

$\boldsymbol{G_{yy}(f)}$ **:** spectral density matrix of the out-put, which has a dimension of **m x m**;

$\boldsymbol{H(f)}$ **:** frequency response functions matrix, which has a dimension of **m x r**.

2.4.6 Frequency response function

As we saw in the second chapter the frequency response function could be written as the ratio between the Fourier Transform of the out-put over the in-put one.

$$\underset{\sim}{H}(\omega) = \frac{Y(\omega)}{X(\omega)}$$

(103)

If we consider the external force like an impulse $f = A \cdot \delta(t)$, la FRF is proportional to $X(\omega)$, apart from an unessential factor:

$$\boldsymbol{x(t)} = \sum_{k=1}^{n} u_k e^{-\zeta_k \omega_k t} (A_k \cos \omega_{kd} t + B_k \sin \omega_{kd} t)$$

(104)

where u_k is the modal constant, ς_k is the damping ratio and $\omega_{kd} = \omega_k \sqrt{1-\xi_k^2}$ is the damping frequency for the k-th mode and A_k, B_k are two constants.

In order to use the FRF in the form of inertance we have to derive the previous equation two times:

$$\boldsymbol{\ddot{x}(t)} = \sum_{k=1}^{n} \omega_k^2 u_k e^{-\zeta_k \omega_k t} (\alpha_k \cos \omega_{kd} t + \beta_k \sin \omega_{kd} t)$$

(105)

where

$$\alpha_k = -2\varsigma_k \sqrt{1-\varsigma_k^2} B_k - (1-2\varsigma_k^2) A_k$$

(106)

$$\beta_k = 2\varsigma_k \sqrt{1-\varsigma_k^2} A_k - (1-2\varsigma_k^2) B_k$$

Applying the Fourier Transform of $\boldsymbol{\ddot{x}(t)}$:

$$\underset{\sim}{H}(\omega) = \sum_{k=1}^{n} u_k \omega_k^2 \frac{\beta_k \omega_{kd} + \alpha_k \varsigma_k \omega_k + \alpha_k i\omega}{(\varsigma_k \omega_k + i\omega)^2 + \omega_{kd}^2}$$

(107)

and supposing

$$\lambda_k = \omega_k(-\varsigma_k + i\sqrt{1-\varsigma_k^2}) = -\sigma_k + i\omega_k$$

(108)

$$\overline{\lambda}_k = \omega_k(-\varsigma_k - i\sqrt{1-\varsigma_k^2}) = -\sigma_k - i\omega_k$$

is it obtained:

$$(\varsigma_k\omega_k + i\omega)^2 + \omega_{kd}^2 = (i\omega - \lambda_k)(i\omega + \lambda_k)$$

(109)

therefore it follows:

$$\underset{\sim}{H}(\omega) = \sum_{k=1}^{n} u_k\omega_k^2 \frac{\beta_k\omega_{kd} + \alpha_k\varsigma_k\omega_k + \alpha_k i\omega}{(s-\lambda_k)(s-\overline{\lambda}_k)}$$

(110)

with $s = i\omega$ and finally grouping together the quantities in the following way:

$$\varphi_k = \frac{1}{2}\alpha_k + i\beta_k$$

$$\overline{\varphi}_k = \frac{1}{2}\alpha_k - i\beta_k$$

$$\underset{\sim}{R}_k = u_k\omega_k^2 G_k = \gamma_k\varphi_k$$

$$\overline{\underset{\sim}{R}}_k = u_k\omega_k^2\overline{G}_k = \gamma_k\overline{\varphi}_k$$

(111)

where φ_k and γ_k are the mode shape vector and the modal participation vector, respectively.

The FRF assumes the expression:

$$\underset{\sim}{H}(\omega) = \sum_{k=1}^{n} \frac{\underset{\sim}{R}_k}{i\omega - \lambda_k} + \frac{\overline{\underset{\sim}{R}}_k}{i\omega - \overline{\lambda}_k}$$

(112)

where $\underset{\sim}{R}_k$ and λ_k are called the residues and the poles respectively. The residue is the product of the eigenvectors.

2.4.7 Decomposition of the Power Spectral Density matrix of the out-put

Supposing the input consists just of the white noise, the corresponding PSD is a constant matrix:

$$\underset{\sim}{\boldsymbol{G}}_{xx}(\omega) = \underset{\sim}{C}$$

(113)

and the PSD of the output could be written as follow:

$$\underset{\sim}{\boldsymbol{G}}_{yy}(\boldsymbol{\omega}) = \sum_{k=1}^{n}\sum_{s=1}^{n}\left[\frac{\underset{\sim}{R}_k}{i\omega-\lambda_k}+\frac{\overline{\underset{\sim}{R}}_k}{i\omega-\overline{\lambda}_k}\right]\cdot\underset{\sim}{C}\cdot\left[\frac{\underset{\sim}{R}_s}{i\omega-\lambda_s}+\frac{\overline{\underset{\sim}{R}}_s}{i\omega-\overline{\lambda}_s}\right]^H$$

(114)

where superscript H denotes a complex conjugate and transpose. Multiplying the two partial fraction factors and making use of the Heaviside partial fraction theorem, after some mathematical manipulations, the output PSD can be reduced to a pole/residue form as follows:

$$\underset{\sim}{\boldsymbol{G}}_{yy}(\boldsymbol{\omega}) = \sum_{k=1}^{n}\frac{\underset{\sim}{A}_k}{i\omega-\lambda_k}+\frac{\overline{\underset{\sim}{A}}_k}{i\omega-\overline{\lambda}_k}+\frac{\underset{\sim}{B}_k}{i\omega-\lambda_k}+\frac{\overline{\underset{\sim}{B}}_k}{i\omega-\overline{\lambda}_k}$$

(115)

where $\underset{\sim}{A}_k$ is the *k*-th matrix of the residues of the output PSD:

$$\underset{\sim}{A}_k = \underset{\sim}{R}_k\underset{\sim}{C}\left[\sum_{s=1}^{n}\frac{\overline{\underset{\sim}{R}}_s^T}{-\overline{\lambda}_k-\overline{\lambda}_s}+\frac{\underset{\sim}{R}_s^T}{-\lambda_k-\lambda_s}\right]$$

(116)

The contribution of the *k*-th mode is given by:

$$\underset{\sim}{A}_k = \frac{\underset{\sim}{R}_k\underset{\sim}{C}\overline{\underset{\sim}{R}}_k^T}{2\sigma_k}$$

(117)

and σ_k comes from the real part of λ_k.

It is clear that the term σ_k becomes dominant if the damping is light:

$$A_k \propto R_k C \overline{R}_k^T = \varphi_k \gamma_k^T C \gamma_k \varphi_k^T = d_k \varphi_k \varphi_k^T \quad (118)$$

where d_k is a constant scalar.

For each frequency just a finite number of modes are dominant, usually one or two. Indicating this group of modes like $Sub(\omega)$, the answer of the system could be written as follow:

$$\underset{\sim}{G}_{yy}(\omega) = \sum_{k \in Sub(\omega)}^{n} \frac{d_k \varphi_k \varphi_k^T}{i\omega - \lambda_k} + \frac{\overline{d}_k \overline{\varphi}_k \overline{\varphi}_k^T}{i\omega - \overline{\lambda}_k} \quad (119)$$

This is the modal decomposition of the spectral matrix. The expression is similar to the result we could obtain directly from this

Implementation of the EFDD method

On the root of this method there is the decomposition of the output in simple one degree of freedom systems SDOF . This decomposition is obtained by selecting the spectral bell close to the peak of interest and corresponding to the k-th mode. We are going to describing the steps of this method.

3.3.1 Filtering

It is often a good idea to filter the input signals with a low-pass and high-pass filter or with a band-pass filter. Filtering concentrates the identification to the frequency range of interest and reduces the effect of high-frequency measurement noise. A data signal normally has a mixture of different frequency components in it. The frequency contents of the signal and its powers can be obtained for example trough the Fast Fourier Transform (FFT).

The low pass filter posses relatively low frequency components in the signal, but stop the high frequency components. The high-pass filter does the contrary. The so-called cut off frequency divides the pass band and the stop band. The high pass filter is

especially useful since the random errors involved in the row position data obtained trough reconstruction are characterized by relatively high frequency contents.

The data records we analyzed were filtered by the *Butterworth filter*, included in Matlab programming software. It is designed to have a frequency response which is as flat as mathematically possible in the pass band. Another name for it is maximally flat magnitude filter. The behaviour of a filter can be summarized by the so-called frequency response function. The FRF of the Butterworth low-pas filter has the following form:

$$\left|\boldsymbol{H}_c(\boldsymbol{i}\omega)\right|^2 = \frac{1}{1+(\boldsymbol{i}\omega/\boldsymbol{i}\omega_c)^{2N}} \tag{120}$$

where ω is the frequency (rad/sec), ω_c is the cut off frequency (rad/sec) and N is the order of the filter. When $\omega = 0$ the magnitude squared function $\boldsymbol{H}_c^{\,2}$ becomes 1 and the frequency components completely passed. When $\omega = \infty$, $\boldsymbol{H}_c^{\,2}$ becomes 0 and the frequency components will be completely stopped. Between the pass band and the stop band there is the transition band $(1 > \boldsymbol{H}_c^{\,2} > 0)$ in which the components will be partially passed but partially stopped at the same time. When $\omega = \omega_c$, $\boldsymbol{H}_c^{\,2}$ always becomes 0,5 (half power regardless of the order of the filter). The things we explained will be clearer looking at the following figure.

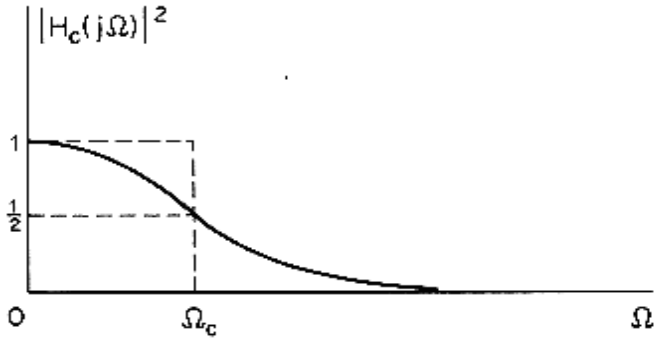

Figure1.26.

1.1 Figure FRF of the low-pass Butterworth filter

Figure1.27. The following figure instead shows the effect of the filter order on the frequency response. As the filter order increase, the transition from the pass band to the stop band gets steeper

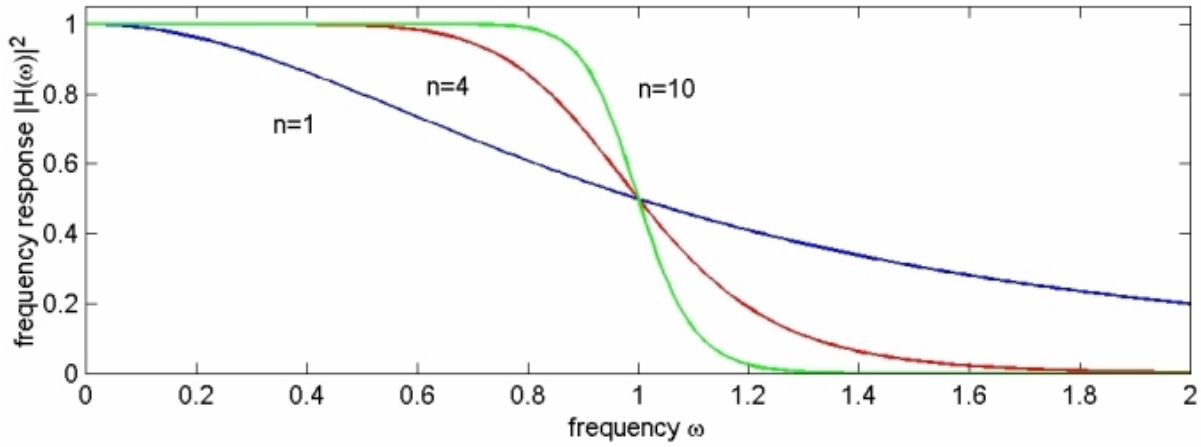

1.2 Figure Effect of the different orders of the filter.

Therefore when the order of the filter is bigger, the filtering effect is better at the cost of longer computational time. On the other hand, a smaller order leads to a shorter computational time and more approximate filtering effect.

In order to filter our data sets we used a 5^{th} order high-pass filter with cut off frequency equal to 0.8 and a 9^{th} order low-pass filter with cut off frequency equal to 15. The frequency range was decided referring to the natural frequencies provided by the FEM model.

3.3.2 Assembly of the power spectral density of the output

For each set of measurements it is valued the PSD matrix that has a dimension of *m* x *m,* where *m* is the numbers of instrument used to collect the data:

$$\underset{\sim}{\boldsymbol{G}}_{\boldsymbol{yy}}(\boldsymbol{f}) = \begin{bmatrix} G_{y_1y_2}(f) & G_{y_1y_2}(f) & \ldots & G_{y_1y_m}(f) \\ G_{y_2y_1}(f) & G_{y_2y_2}(f) & \ldots & G_{y_2y_m}(f) \\ \ldots & \ldots & \ldots & \\ G_{y_my_1}(f) & G_{y_my_2}(f) & \ldots & G_{y_my_m}(f) \end{bmatrix}$$

(121)

where $G_{y_iy_i}(f)$ is auto-spectrum density function, and $G_{y_iy_j}(f)$ is the cross-spectrum density function. Two different approaches were used to obtain this matrix.

1. Valuation of PSD matrix passing for the FFT of each data.
2. Valuation of the CPSD matrix of the data.

1) As we saw in the second chapter the fast Fourier transformation of the autocorrelation function $R_{yy}(\tau)$ is called spectral density power function (PSD), or auto-spectrum:

$$\boldsymbol{S}_{\boldsymbol{yy}}(\omega) = \int_{-\infty}^{+\infty} \boldsymbol{R}_{\boldsymbol{yy}}(\tau)\boldsymbol{e}^{-j2\pi\omega\tau}\mathrm{d}\tau$$

(122).

The function $S_{xx}(\omega)$ is obtained by the Fourier transformation $Y(\omega)$ of the time history $y(t)$. Therefore the first step is to compute the N-points FFT for each set of data $\boldsymbol{Y}(\boldsymbol{f}_{\boldsymbol{k}})$, $\boldsymbol{k} = 0....(\boldsymbol{N}-1)$, where N is number of the data values.

Form the Fourier transform it is possible to find the one-side auto-spectral and cross-spectral density function of the signals:

$$G_{y_iy_i} = \frac{2}{\Delta t \cdot N}\left|Y_i\right|^2$$

(123)

$$G_{y_iy_i} = \frac{2}{N \cdot \Delta t}\left|\overline{Y}_j Y_i\right| \qquad i \neq j$$

(124)

where Δt is the sampling time.

Anyway the plot of the PSD showed still a not clearly of the peaks. Therefore another approach was used.

2) Calculation of the CPSD using the Matlab function

[Pxy,F] = cpsd(x,y,window,noverlap,nfft,fs).

This function, based on the cross-spectrum power density function, requires the division of the data signals in sequences, their windowing and overlapping. We will show the steps of the method.

In order to get the CPSD we have to divide the available data records for $x_i(t)$ and $y_i(t)$ into n_d pairs of blocks, each consisting of *N* data values.

$$x_i(t) = x_1 \cup x_2 \cup ... \cup x_n$$

(125)

$$y_i(t) = y_1 \cup y_2 \cup ... \cup y_n$$

Figure1.28.

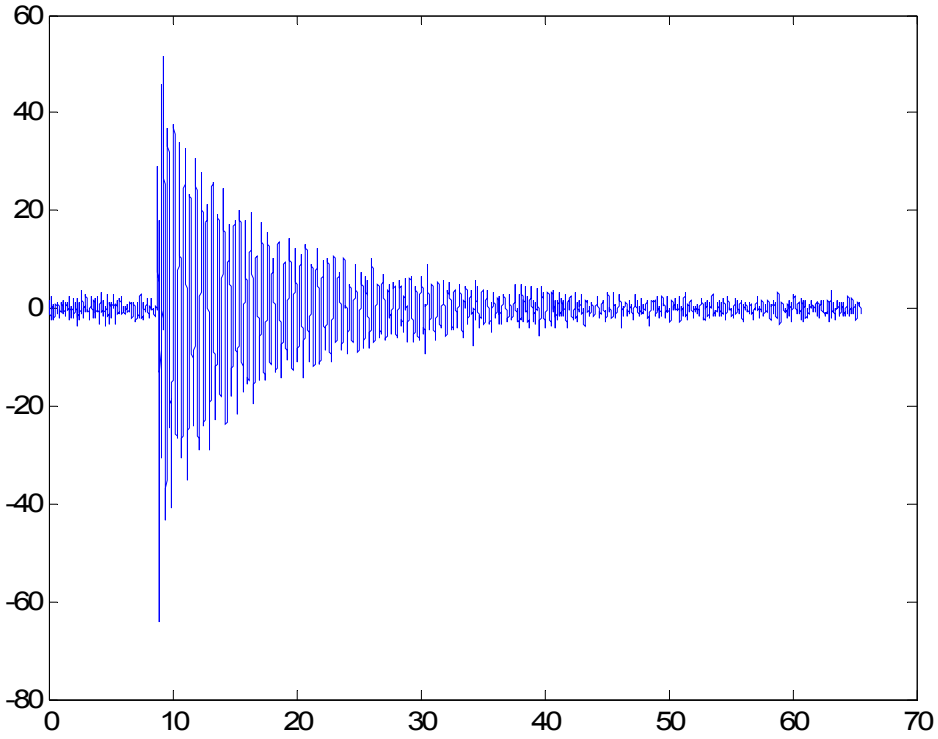

Figure1.29.

Figure1.30.

Figure1.31.

Figure1.32.

Figure1.33.

Figure1.34.

Figure1.35.

Figure1.36.

Figure1.37.

Figure1.38.

1.3 Figure division in sequences and overlapping of the data records

Each block is traded separately and with the averaged value centred to zero, therefore cleared off possible trends. After that the signals are multiply for the windowing function called Hanning window W that help to reduce the leakage problems:

$$\hat{x}_k = x_k \cdot W \quad , \qquad \hat{y}_k = y_k \cdot W$$

where the symbol " ^ ", stands for windowed.

This function removes the codes of the sequence in consideration using a window as we showed in the previous chapter and it might assume also different length despite of the sequence (usually shorter) and in this case a finite number of zeros are added to the signals. The mathematical expression of the Hanning window is the following:

$$W(t) = 1 - \left(\cos \frac{\pi r}{s} \right)^2 \qquad r = 0,1,2,.....,s$$
$$W(t) = 0 \qquad\qquad\qquad\qquad r > s$$

(126)

where s represents the width, in samples, of a discrete-time window function and r is an integer $0 < r \le s$.

For each sequence windowed and overlapped, is it valued the Discrete Fourier Transform (DFT):

$$\begin{aligned}
&\hat{x}_1 \leftrightarrow \hat{X}_1 \qquad && \hat{y}_1 \leftrightarrow \hat{Y}_1 \\
&\hat{x}_2 \leftrightarrow \hat{X}_2 \qquad && \hat{y}_2 \leftrightarrow \hat{Y}_2 \\
&\ldots \qquad && \ldots \\
&\hat{x}_k \leftrightarrow \hat{X}_k \qquad && \hat{y}_k \leftrightarrow \hat{Y}_k \\
&\ldots \qquad && \ldots \\
&\hat{x}_n \leftrightarrow \hat{X}_n \qquad && \hat{y}_n \leftrightarrow \hat{Y}_n
\end{aligned}$$

(127)

Moreover the transforms are averaged as follow:

$$Y_i = \sum_{k=1}^{n} \hat{Y}_k \quad \text{and} \quad X_i = \sum_{k=1}^{n} \hat{X}_k$$

(128)